(2)

Report No. NADC-88118-60

A NEW APPROXIMATE FRACTURE MECHANICS ANALYSIS METHODOLOGY FOR COMPOSITES WITH A CRACK OR HOLE

Hsi C. Tsai and Annette M. Arocho
Air Vehicle And Crew Systems Technology Department (Code 6043)
NAVAL AIR DEVELOPMENT CENTER
Warminster, PA 18974-5000

30 APRIL 1990

PHASE REPORT
Period Covering October 1986 to September 1988
Task No. R02303001
Work Unit No. 133126
Program Element No. 601153N
Project No. BR-23-03-01

Approved for Public Release; Distribution is Unlimited

Prepared for
NAVAL AIR SYSTEMS COMMAND (AIR-931B)
Washington, DC 20361-0001

NOTICES

REPORT NUMBERING SYSTEM — The numbering of technical project reports issued by the Naval Air Development Center is arranged for specific identification purposes. Each number consists of the Center acronym, the calendar year in which the number was assigned, the sequence number of the report within the specific calendar year, and the official 2-digit correspondence code of the Command Officer or the Functional Department responsible for the report. For example: Report No. NADC-88020-60 indicates the twentieth Center report for the year 1988 and prepared by the Air Vehicle and Crew Systems Technology Department. The numerical codes are as follows:

CODE	OFFICE OR DEPARTMENT
00	Commander, Naval Air Development Center
01	Technical Director, Naval Air Development Center
05	Computer Department
10	AntiSubmarine Warfare Systems Department
20	Tactical Air Systems Department
30	Warfare Systems Analysis Department
40	Communication Navigation Technology Department
50	Mission Avionics Technology Department
60	Air Vehicle & Crew Systems Technology Department
70	Systems & Software Technology Department
80	Engineering Support Group
90	Test & Evaluation Group

PRODUCT ENDORSEMENT — The discussion or instructions concerning commercial products herein do not constitute an endorsement by the Government nor do they convey or imply the license or right to use such products.

Reviewed By: A. Manny Date: 1/7/91
Branch Head

Reviewed By: Abert C. Huang Date: 1/14/91
Division Head

Reviewed By: W. J. Smith Date: 1/15/91
Director/Deputy Director

REPORT DOCUMENTATION PAGE

Form Approved
OMB No 0704-0188

1a REPORT SECURITY CLASSIFICATION UNCLASSIFIED	1b RESTRICTIVE MARKINGS
2a SECURITY CLASSIFICATION AUTHORITY	3 DISTRIBUTION / AVAILABILITY OF REPORT Approved for Public Release; Distribution is Unlimited
2b DECLASSIFICATION / DOWNGRADING SCHEDULE	
4. PERFORMING ORGANIZATION REPORT NUMBER(S) NADC-88118-60	5 MONITORING ORGANIZATION REPORT NUMBER(S)
6a NAME OF PERFORMING ORGANIZATION Air Vehicle and Crew Systems Technology Department; 6b OFFICE SYMBOL (If applicable) 6043	7a. NAME OF MONITORING ORGANIZATION
6c. ADDRESS (City, State, and ZIP Code) NAVAL AIR DEVELOPMENT CENTER Warminster, PA 18974-5000	7b ADDRESS (City, State, and ZIP Code)
8a. NAME OF FUNDING / SPONSORING ORGANIZATION NAVAL AIR SYSTEMS COMMAND; 8b OFFICE SYMBOL (If applicable)	9 PROCUREMENT INSTRUMENT IDENTIFICATION NUMBER
8c. ADDRESS (City, State, and ZIP Code) Washington DC 20361-0001	10 SOURCE OF FUNDING NUMBERS: PROGRAM ELEMENT NO; PROJECT NO; TASK NO; WORK UNIT ACCESSION NO

11. TITLE (Include Security Classification)
A New Approximate Fracture Mechanics Analysis Methodology for Composites with a Crack or Hole

12. PERSONAL AUTHOR(S) Hsi Chin Tsai and Annette M. Arocho

13a TYPE OF REPORT	13b TIME COVERED	14 DATE OF REPORT (Year, Month, Day)	15 PAGE COUNT
Phase	FROM 10/86 TO 9/88	1990 April 30	

16 SUPPLEMENTARY NOTATION

17 COSATI CODES			18 SUBJECT TERMS (Continue on reverse if necessary and identify by block number)
FIELD	GROUP	SUB-GROUP	Equivalent stress intensity factor, Bi-Material Interface, Inherent flaw, Microscopic Model, Anisotropic Model, Fracture Mechanics, Composites

19 ABSTRACT (Continue on reverse if necessary and identify by block number)

A new approximate theory which links the inherent flaw concept and the theory of crack tip stress singularities at a bi-material interface has been developed. Three assumptions were made: (1) the existence of inherent flaw (i.e., damage zone) at the tip of the crack was postulated, (2) a fracture of the filamentary composites initiates at a crack lying in the matrix material at the interface of the matrix/filament, (3) a laminate fails whenever the principal load-carrying laminae fails. This will imply that for a laminate consisting of 0° plies, cracks in the matrix perpendicular to the 0° filaments are the triggering mechanism for the final failure.

Based on this theory, a parameter $\bar{K}_Q$ which is similar to the stress intensity factor defined for isotropic materials but with a different dimension was defined. Utilizing existing test data, it was found that $\bar{K}_Q$ can be treated as material constant. Based on this finding a fracture strength prediction methodology was developed.

The analytical results are correlated well with the test results. This new approximate theory can apply to both brittle and metal matrix composite laminates with crack or hole.

20 DISTRIBUTION / AVAILABILITY OF ABSTRACT ☒ UNCLASSIFIED/UNLIMITED ☐ SAME AS RPT ☒ DTIC USERS	21 ABSTRACT SECURITY CLASSIFICATION
22a NAME OF RESPONSIBLE INDIVIDUAL Hsi Chin Tsai	22b TELEPHONE (Include Area Code) 215-441-2871; 22c OFFICE SYMBOL 6043

CONTENTS

CONTENTS (Continued)

THIS PAGE INTENTIONALLY LEFT BLANK

FIGURES

FIGURES (Continued)

TABLES

SYMBOLS

σ_N — gross nominal stress

σ_0 — unnotched strength of a composite laminate

R_0 — radius of a hole

a_0 — half crack length

w — width of laminate

r — radius from crack tip

θ — angle measured from x-axis

K — stress intensity factor for isotropic materials

Y — finite width plate correction factor

m — order of singularity

$\overline{K}$ — the equivalent stress intensity factor for composite material

$\overline{K}_{AVG}$ — average value of $\overline{K}$ from a material of all the crack sizes

$\overline{K}_Q$ — critical equivalent stress intensity factor

$\overline{K}_{LSF}$ — $\overline{K}$ derived from C_0 based on least square fit

α — composite parameter

β — composite parameter

ν_1, ν_2 — poison ratio for medium 1 and 2 respectively

μ_1, μ_2 — shear modulus for medium 1 and 2 respectively

C_0 — inherent flaw size

ξ — $\dfrac{2a_0}{w}$

C_0^* — Inherent flaw size corresponding to an anisotropic model

THIS PAGE INTENTIONALLY LEFT BLANK

1.0 INTRODUCTION

The failure modes associated with fractures in fiber-reinforced composites differ considerably from those of homogeneous isotropic materials. The failure modes in composites are typically in the forms of transverse cracking, delamination, fiber breaks, matrix yielding, matrix cracking, fiber pull-out and fiber/matrix debonding. As a result, it is a very difficult task to predict the fracture process and behavior of composite materials exactly.

In the past, a great deal of effort has been expended to investigate the fracture behavior of composites. A number of fracture mechanics theories have been proposed. These theories have been reviewed and presented extensively in References 1 and 2.

In this report a microscopic theory which was originally proposed by Mar and Lin[9] has been modified into a new theory. This new theory links the inherent flaw concept[3-8], which postulates that a damage zone exists at the tip of crack, and the theory of crack singularities at a bi-material interface[9-12]. This combined theory can be used to predict the notched strength of organic and metal matrix composites with either a crack or a hole.

The following sections of this report describe the methodology used in the analysis, assumptions taken, analytical results obtained and conclusions made.

2.0 THEORY

The stress distribution at the crack tip in a thin plate for a homogeneous, isotropic elastic solid in terms of the coordinates shown in Figure 1 is given by equation (1)

$$\sigma_x = \sigma_N \left(\frac{a_o}{2r}\right)^{1/2} \left[\cos\frac{\theta}{2}\left(1 - \sin\frac{\theta}{2}\sin\frac{3\theta}{2}\right)\right]$$

$$\sigma_y = \sigma_N \left(\frac{a_o}{2r}\right)^{1/2} \left[\cos\frac{\theta}{2}\left(1 + \sin\frac{\theta}{2}\sin\frac{3\theta}{2}\right)\right]$$

$$\tau_{xy} = \sigma_N \left(\frac{a_o}{2r}\right)^{1/2} \left[\sin\frac{\theta}{2}\cos\frac{\theta}{2}\cos\frac{3\theta}{2}\right] \tag{1}$$

where

σ_N = gross nominal stress.

For an orientation directly ahead of the crack ($\theta = 0$)

$$\sigma_x = \sigma_y = \sigma_N \left(\frac{a_o}{2r}\right)^{1/2} \quad \text{and} \quad \tau_{xy} = 0 \tag{2}$$

Irwin[13] pointed out that equation (1) indicates that the local stresses near a crack depend on the product of the nominal stress and the square root of the half-flaw length. He called this relationship the stress intensity factor K, where for a sharp elastic crack in an infinitely wide plate, K is defined as

$$K = \sigma_N \sqrt{a_o} \tag{3}$$

In the approach using linear-elastic fracture mechanics (LEFM), K is a material parameter and may be determined from tests.

For a finite-width plate, equation (3) is modified to

$$K = Y \sigma_N \sqrt{a_o} \tag{4}$$

Where Y is a parameter that depends on the plate and crack geometry.

To develop a similar concept for composite materials, the assumptions of references 3, 9 were adopted in this paper; i.e.:

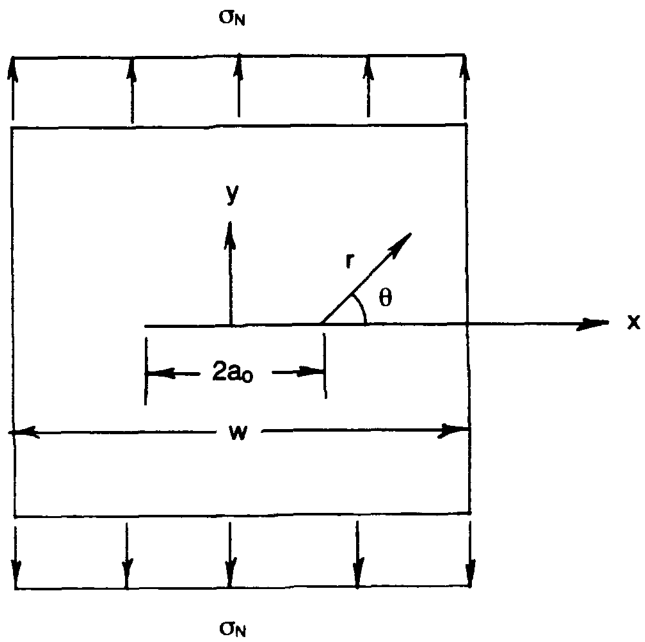

Figure 1. Model For Equations For Stresses At A Point Near A Crack.

- The existence of an inherent flaw (also called a damage zone) at the edge of a hole or at the tip of a crack.
- Fracture of a filamentary composite initiates at a crack lying in the matrix material at the interface of the matrix/filament.
- A laminate fails whenever the principal load-carrying laminae fails. This implies that cracks in the matrix perpendicular to the 0° filaments are the triggering mechanism for the final failure.

Based on the above assumptions, the following theories are developed:

Using the same concept of stress intensity factor as is formulated above for isotropic materials, a material parameter similar to K is defined for composite material as:

$$\bar{K} = Y\sigma_N (a_o)^m \tag{5}$$

where m is the order of singularity of a crack whose tip is at the interface of two different materials as shown in Figure 2. Calculations for determining m are presented in Reference 18.

Note that $\bar{K}$ has a different dimension from K. (K has a dimension of "stress times length to the 1/2 power", while $\bar{K}$ has a dimension of "stress times length to the m power".)

Although some composite materials (such as polymeric matrix composites) fail in a brittle manner, a damage zone does develop which is analogous to the plastic zone for ductile materials. Using this concept in conjunction with equation (5) yields:

$$\bar{K} = Y\sigma_N (a_o + C_o)^m \tag{6}$$

where C_o is defined as an inherent flaw size. The term inherent flaw size is used since unnotched strength, σ_o, of a composite laminate is given by equation (6) for the case of vanishing a_o,

$$\bar{K} = \sigma_o (C_o)^m \tag{7}$$

where Y_o is the correction factor for infinite plate.

It should be noted that C_o does not physically refer to an inherent crack, but a characteristic dimension of damage zone at the tip of a notch or crack prior to ultimate failure.

The question we may ask now is whether $\bar{K}$ and C_o are material constants. Before we reach a conclusion, certain equations are helpful in answering this question.

Substituting equation (7) into equation (6), and after some manipulations, we obtain the following important equations that will be used to determine parameter $\bar{K}$, C_o and notched strength of composite laminates

$$C_o = \frac{a_o}{\left(\frac{\sigma_o}{\bar{Y}\sigma_N}\right)^{1/m} - 1} \tag{8}$$

$$\bar{K} = a_o^m Y_o \sigma_o \left\{\left(\frac{\bar{Y}\sigma_N}{\sigma_o}\right)^{-1/m} - 1\right\}^{-m} \tag{9}$$

$$\frac{\sigma_N}{\sigma_o} = \frac{1}{\bar{Y}}\left\{\frac{C_o}{a_o + C_o}\right\}^m \tag{10}$$

or

$$\frac{\sigma_N}{\sigma_o} = \frac{1}{\bar{Y}} \frac{1}{\left\{1 + \left(\frac{Y_o\sigma_o}{\bar{K}}\right)^{\frac{1}{m}} a_o\right\}^m} \tag{11}$$

where

$$\bar{Y} = \frac{Y}{Y_o}$$

In the following sections, $\bar{K}$ will be called the equivalent stress intensity factor for composite materials.

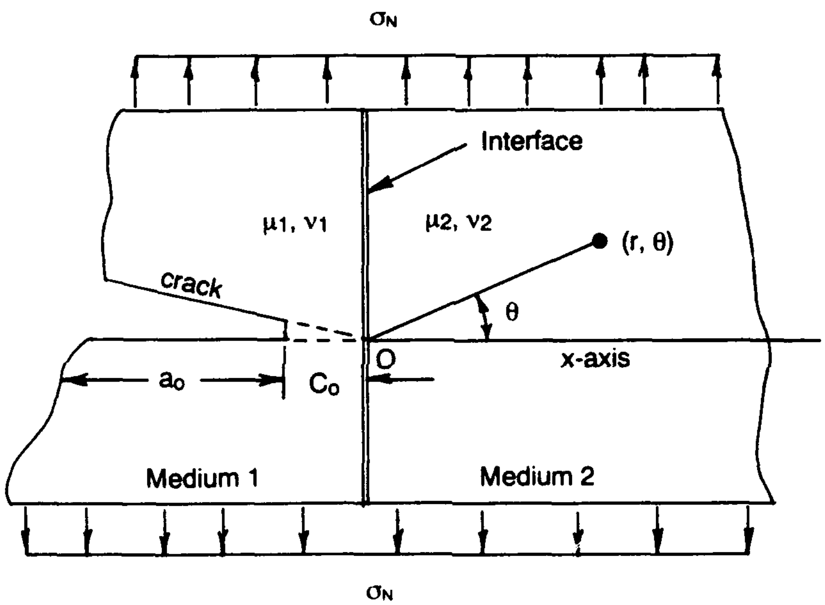

Figure 2. Crack Normal To The Bi-Material Interface With Inherent Flaw, C_o.

3.0 DETERMINATION OF EQUIVALENT STRESS INTENSITY FACTOR, $\overline{K}$ AND INHERENT FLAW SIZE

Reference 8 provides extensive fracture test data of boron/aluminum laminates with various proportions of 0° and ±45° plies. Hence. this test data will be used to characterize the fracture behavior of boron/aluminum composite laminates.

3.1 EQUIVALENT STRESS INTENSITY FACTOR, $\overline{K}$

From Appendix A, the order of stress singularity at the boron/aluminum interface, m equals .347. From equation (9), the equivalent stress intensity factor for boron/aluminum composite laminate with center crack can be written as follows:

$$\overline{K} = a_o^{.347}\sigma_o\left\{\left(\frac{Y\sigma_N}{\sigma_o}\right)^{-2.88} - 1\right\}^{-.347} \tag{12}$$

Equation (12) is used to characterize the critical equivalent stress intensity factor of boron/aluminum laminates with various layups.

By using the fracture test results from reference 8, equivalent stress intensity factors were calculated from equation (12) and are tabulated on Tables 1 through 4 for boron/aluminum composite with laminate constructions $[0]_{6T}$. $[0_2/\pm45]_s$, $[\pm45/02]_s$ and $[0/\pm45]_s$ respectively. Note the test results shown in Tables 1 to 4 are average test results of reference 8. As shown in Tables 1 to 4, $\overline{K}$ values seem to be a material property and vary with different laminate orientations. $\overline{K}$ values are also plotted on Figures 3 to 6. $\overline{K}_{AVG}$ is the average value of $\overline{K}$ from all the crack sizes. As shown in the figures, $\overline{K}_{AVG}$ can be approximately treated as a material constant. It has to be pointed out here that $\overline{K}_{AVG}$ was obtained by averaging three different widths of plate. For w = 101.6mm $\overline{K}$ values are almost the same for different $2a_o/w$ ratios.

The detailed calculations of $\overline{K}$ are shown in Appendix B.1.

Table 1. Equivalent Stress Intensity Factor For $[0]_{6T}$ B/Al Composite.

w (mm)	a_o (mm)	ξ	Y	$\left(\frac{\sigma_N}{\sigma_o}\right)_{TEST}$	$\bar{K}$ (MPa(mm)$^{.347}$)	$\left(\frac{\sigma_N}{\sigma_o}\right)$	Error %
19.1	.25	.025	1.001	.818	1125.0	.878	7.4
19.1	.65	.068	1.003	.6845	1136.0	.760	11.0
50.8	1.25	.05	1.001	.592	1166	.663	12.0
50.8	2.55	.1	1.006	.555	1455	.546	−1.6
50.8	7.6	.3	1.06	.4003	1479	.3705	−7.5
50.8	12.7	.5	1.189	.3098	1518	.279	−10.0
101.6	2.55	.05	1.001	.580	1455	.549	−5.3
101.6	5.1	.1	1.006	.468	1435	.443	−5.3
101.6	15.25	.3	1.06	.3024	1399	.295	−2.6
101.6	25.4	.5	1.189	.232	1430	.221	−4.7

$$\bar{K}^{AVG} = 1360 \text{ MPa (mm)}^{.347}$$

$$\sigma_o = 1672 \text{ MPa}$$

$$Y = \sqrt{\sec\left(\frac{\pi}{2}\xi\right)}$$

$$\xi = \frac{2a_o}{w}$$

Table 2. Equivalent Stress Intensity Factor For $[0_2/\pm 45]_s$ B/Al Composite.

w (mm)	a_0 (mm)	ξ	Y	$\left(\frac{\sigma_N}{\sigma_0}\right)_{TEST}$	$\overline{K}$ (MPa(mm)$^{.347}$)	$\left(\frac{\sigma_N}{\sigma_0}\right)$	Error %
19.1	.25	.025	1.001	.878	652.6	.891	1.5
19.1	.65	.068	1.003	.782	681.9	.782	0.
50.8	1.25	.05	1.001	.721	740.	.686	–4.8
50.8	2.55	.1	1.006	.571	683.1	.570	0.
50.8	7.6	.3	1.06	.395	697.8	.389	–1.5
50.8	12.7	.5	1.189	.274	639.0	.293	7.0
101.6	2.55	.05	1.001	.579	695.1	.572	–1.2
101.6	5.1	.1	1.006	.464	680.6	.464	0.
101.6	15.25	.3	1.06	.321	711.5	.310	–3.5
101.6	25.4	.5	1.189	.229	674.6	.232	1.6

$$\overline{K}^{AVG} = 685.6 \text{ MPa (mm)}^{.347}$$

$$\sigma_0 = 800.1 \text{ MPa}$$

$$Y = \sqrt{\sec\left(\frac{\pi}{2}\xi\right)}$$

$$\xi = \frac{2a_0}{w}$$

Table 3. Equivalent Stress Intensity Factor For $[\pm 45/02]_s$ B/Al Composite.

w (mm)	a_o (mm)	ξ	Y	$\left(\frac{\sigma_N}{\sigma_o}\right)_{TEST}$	$\bar{K}$ (MPa(mm)$^{.347}$)	$\left(\frac{\sigma_N}{\sigma_o}\right)$	Error %
19.1	.25	.025	1.001	–	–	–	–
19.1	.65	.068	1.003	–	–	–	–
50.8	1.25	.05	1.001	.619	674.7	.633	2.3
50.8	2.55	.1	1.006	.531	716.6	.517	–2.6
50.8	7.6	.3	1.06	.361	720.8	.349	–3.5
50.8	12.7	.5	1.189	.245	647.7	.262	7.0
101.6	2.55	.05	1.001	.528	707.6	.520	–1.6
101.6	5.1	.1	1.006	.423	703.8	.417	–1.3
101.6	15.25	.3	1.06	.281	706.2	.276	–1.6
101.6	25.4	.5	1.189	.201	673.0	.207	3.1

$$\bar{K}^{AVG} = 693.8 \text{ MPa(mm)}^{.347}$$

$$\sigma_o = 910.5 \text{ MPa}$$

$$Y = \sqrt{\sec\left(\frac{\pi}{2}\xi\right)}$$

$$\xi = \frac{2a_o}{w}$$

Table 4. Equivalent Stress Intensity Factor For $[0/\pm45]_s$ B/Al Composite.

w (mm)	a_o (mm)	ξ	Y	$\left(\frac{\sigma_N}{\sigma_o}\right)_{TEST}$	$\overline{K}$ $(MPa(mm)^{.347})$	$\left(\frac{\sigma_N}{\sigma_o}\right)$	ERROR %
19.1	.25	.025	1.001	–	–	–	–
19.1	.65	.068	1.003	.828	564.6	.865	4.4
50.8	1.25	.05	1.001	.796	645.8	.789	–1.0
50.8	2.55	.1	1.006	.730	710.1	.688	–5.7
50.8	7.6	.3	1.06	.458	597.8	.481	5.2
50.8	12.7	.5	1.189	.329	563.1	.367	11.5
101.6	2.55	.05	1.001	.699	656.5	.692	–1.0
101.6	5.1	.1	1.006	.620	702.0	.569	–8.2
101.6	15.25	.3	1.06	.413	678.0	.388	–6.0
101.6	25.4	.5	1.189	.271	583.9	.293	8.2

$$\overline{K}^{AVG} = 633.5\ MPa(mm)^{.347}$$

$$\sigma_o = 581.4\ MPa$$

$$Y = \sqrt{\sec\left(\frac{\pi}{2}\xi\right)}$$

$$\xi = \frac{2a}{w}$$

The above tests are for center crack specimens. For other crack types and locations[5], the calculated equivalent stress intensity factors are shown on Table 5, condensed from Appendix B.1.2. It can be seen that $\overline{K}$ for these unidirectional boron/aluminum composites is constant for different crack conditions. The reason for the slightly different K as compared to Table 1 is due to a different value of ultimate tensile strength.

Table 5. Critical Equivalent Stress Intensity Factor Of Unidirectional B/Al[5] Composite.

SPECIMEN*	$\frac{2a_o}{w}$ or $\frac{2R}{w}$	$\overline{K}_{AVG}$ MPa (mm)$^{.347}$
CH	.25	1246.00
CS	.40	1227.00
DEN	.30	1237.00

***CH - CENTER HOLE SPECIMEN**
CS - CENTER SPLIT SPECIMEN
DEN - DOUBLE EDGE NOTCH SPECIMEN

3.2 INHERENT FLAW SIZE, C_O

Two methods were used to calculate the inherent flaw sizes for a composite laminate with center crack.

Least Square Fit

Equation (8), in which C_O is a proportional constant, can be rearranged to yield

$$a_o = C_o\left\{\left(\frac{Y\sigma_N}{\sigma_o}\right)^{-2.88} - 1\right\} \qquad (13)$$

By using the fracture test data as shown in Tables 1 to 4, and the least square fit, C_O for various laminate constructions are determined as shown in Table 6.

Average Equivalent Stress Intensity Method

From Equation (7) we have

$$\overline{K}_{AVG} = \sigma_o\,(C_o)^m \qquad (14)$$

where m = .347 for boron/aluminum.

The inherent flaw size can be derived from equation (14) as follows:

$$C_O = \left(\frac{\overline{K}_{AVG}}{\sigma_O}\right)^{1/m} \tag{15}$$

In the case of boron/aluminum composite, equation (15) becomes

$$C_O = \left(\frac{\overline{K}_{AVG}}{\sigma_O}\right)^{2.88} \tag{16}$$

The inherent flaw sizes for various laminate orientations were calculated using this method and were also tabulated on Table 6.

Table 6. Inherent Flaw Size, C_O (mm).

	Least Square Fit	$\overline{K}_{AVG}$ Method
$[0]_{6T}$	.633	.552
$[0_2/\pm45]_S$	.593	.641
$[\pm45/0_2]_S$	.405	.457
$[0/\pm45]_S$	.976	1.28

We pointed out earlier that C_O does not physically refer to an inherent crack, but rather to a characteristic dimension of damage zone at a crack tip, prior to fracture failure. Comparing the dimension of C_O with respect to the crack size of B/Al specimens as shown in Table 1 to 4, it is clear that C_O cannot be neglected in the calculations of equivalent stress intensity factor. The significance of C_O will be further discussed in Section 4.0.

Equation (7) is used to calculate critical equivalent stress intensity factor based on the C_O determined from least square fit method. These values are also plotted on Figures 3 to 6 as $\overline{K}_{LSF}$. It can be seen from the plots that there is not much difference between $\overline{K}_{LSF}$ and $\overline{K}_{AVG}$ except in the plot for the $[0/\pm45]_S$ laminates, where though there is a greater difference between $\overline{K}_{AVG}$ and $\overline{K}_{LSF}$, $\overline{K}_{AVG}$ provides a better result. For this reason $\overline{K}_{AVG}$ will be adopted in this report and will be denoted as $\overline{K}_Q$.

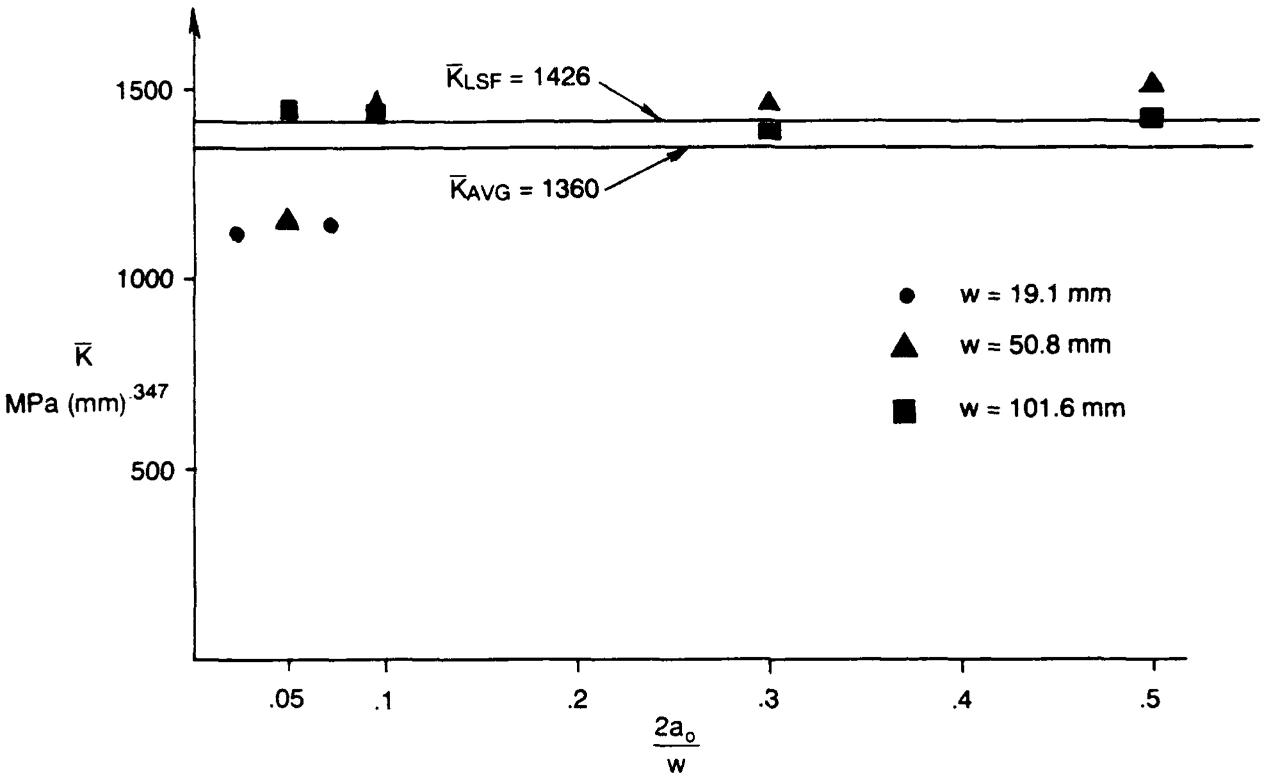

Figure 3. Equivalent Stress Intensity Factor For $[0]_{6T}$ B/Al Composite.

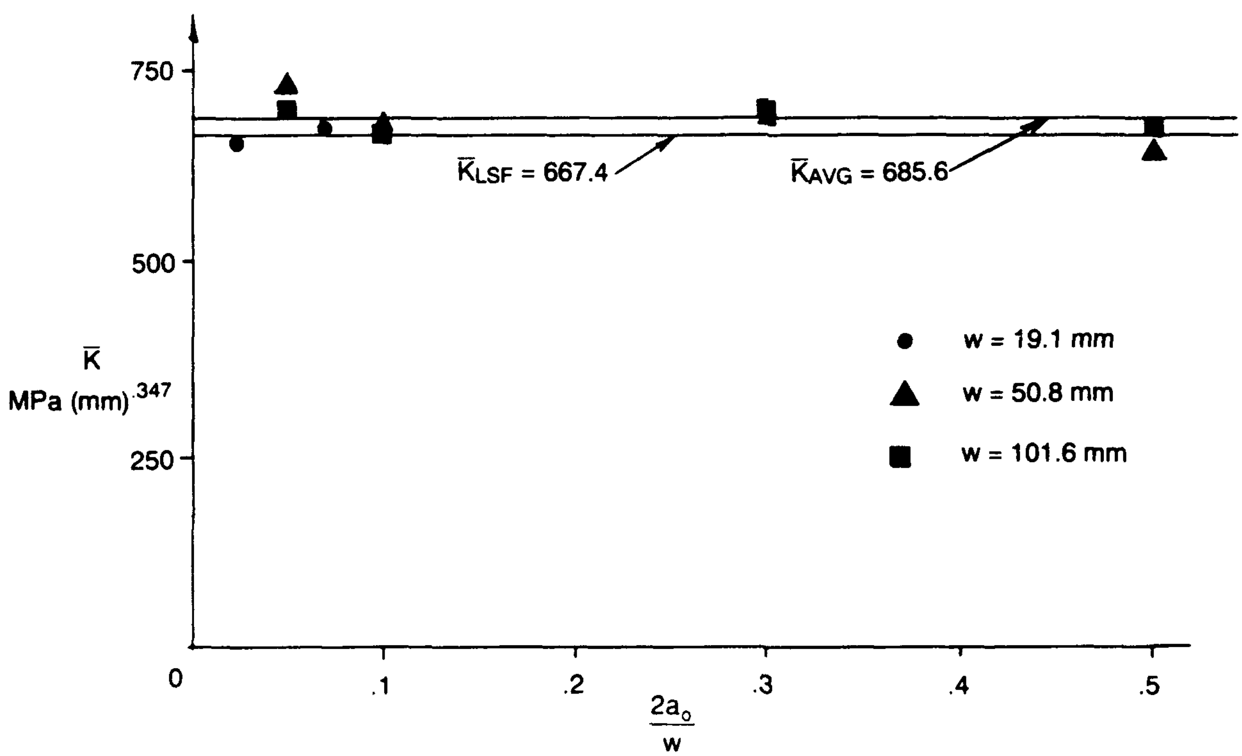

Figure 4. Equivalent Stress Intensity Factor For $[0_2/\pm45]_s$ B/Al Composite.

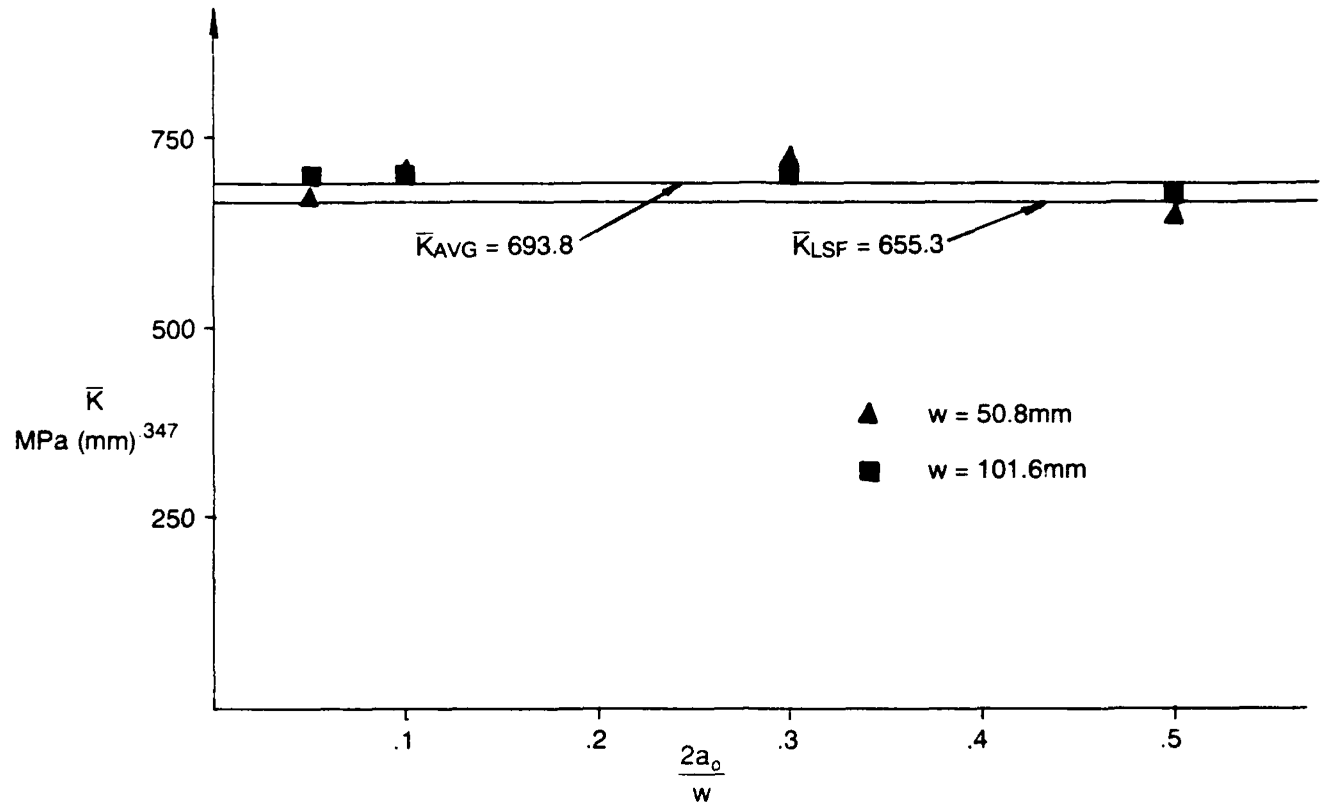

Figure 5. Equivalent Stress Intensity Factor For $[\pm 45/0_2]_s$ B/Al Composite.

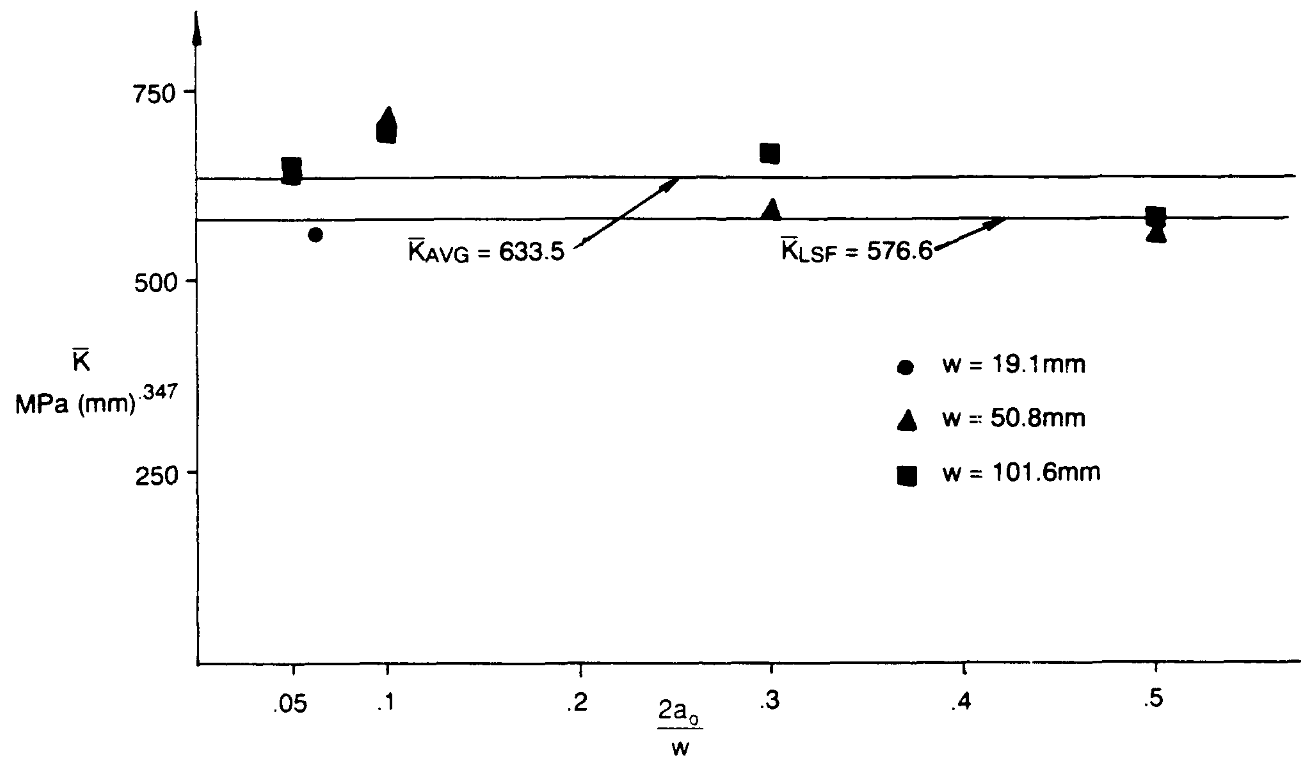

Figure 6. Equivalent Stress Intensity Factor For $[0/\pm 45]_s$ B/Al Composite.

THIS PAGE INTENTIONALLY LEFT BLANK

4.0 APPLICATIONS

Once the critical equivalent stress intensity factor, $\overline{K}_Q$ is known, the fracture strength of the composite laminates can be obtained from equations (10) and (11).

From equation (11), we have a fracture strength prediction formula as follows:

$$\frac{\sigma_N}{\sigma_o} = \frac{1}{Y}\left\{1+\left(\frac{\overline{K}_Q}{Y_o\,\sigma_o}\right)^{-\frac{1}{m}} a_o\right\}^{-m} \tag{17}$$

From Equation (17), it can be seen that the larger the term $\left(\frac{\overline{K}_Q}{\sigma_o}\right)$, the lesser the notch sensitivity and so from equation (7), we can conclude that the larger the inherent flaw size (i.e., the damage zone size), C_o, the lesser the notch sensitivity.

In the following subsections, the theory developed here will be used to predict the fracture strength of various composite laminates.

4.1 BORON/ALUMINUM (B/Al) COMPOSITE

4.1.1. Notched Strength Prediction

For B/Al composite laminates, m = .347 and for a center crack specimen, equation (17) becomes

$$\frac{\sigma_N}{\sigma_o} = \frac{1}{Y}\left\{1+\left(\frac{\overline{K}_Q}{\sigma_o}\right)^{-2.88} a_o\right\}^{-.347} \tag{18}$$

where for a composite laminate with a center crack, Y is assumed to be the same as that for an isotropic material[8].

$$Y = \left\{\sec\left(\frac{\pi a_o}{w}\right)\right\}^{1/2}$$

For convenience, data from Tables 1 to 4 and 6 are summarized on Table 7 to be used for the following analysis. Substituting σ_o and $\overline{K}_Q$ from Table 7 for different ply conditions into equation (18) values for $\frac{\sigma_N}{\sigma_o}$ can be obtained for various crack sizes and are tabulated on Column 7 of Tables 1 to 4. The analytical results are also plotted on Figures 7 to 10.

As can be seen, the prediction represents the experimental results reasonably well.

The $\overline{K}_Q$ values obtained from center cracked specimens are also applied to B/Al specimens with center holes. Comparisons of the analytical results and test results[14] are shown in Figures 11 to 13. Figure 11 shows excellent correlation between test and analytical results for $[0]_{6T}$ laminates with center holes, while in Figure 12 and 13, the maximum percentage error for analytical results is around 13%. The detailed calculations are shown in Appendiz B.1.3. This confirms the findings of reference 18 and 19 that the length of discontinuity and not the shape appeared to control the fracture strength of composite laminates.

Table 7. Fracture Parameters For Various Laminate Configurations Of B/Al.

Ply Configuration	σ_o (MPa)	$\overline{K}_Q$ MPa (mm)$^{.347}$	$\frac{\overline{K}_Q}{\sigma_o}$ (mm)$^{.347}$	C_o (mm)
$[0]_{6T}$	1672	1360	.81	.552
$[0_2/\pm45]_s$	800.1	685.6	.867	.641
$[\pm45/0_2]_s$	910.5	693.8	.762	.457
$[0/\pm45]_s$	581.4	633.5	1.09	1.28

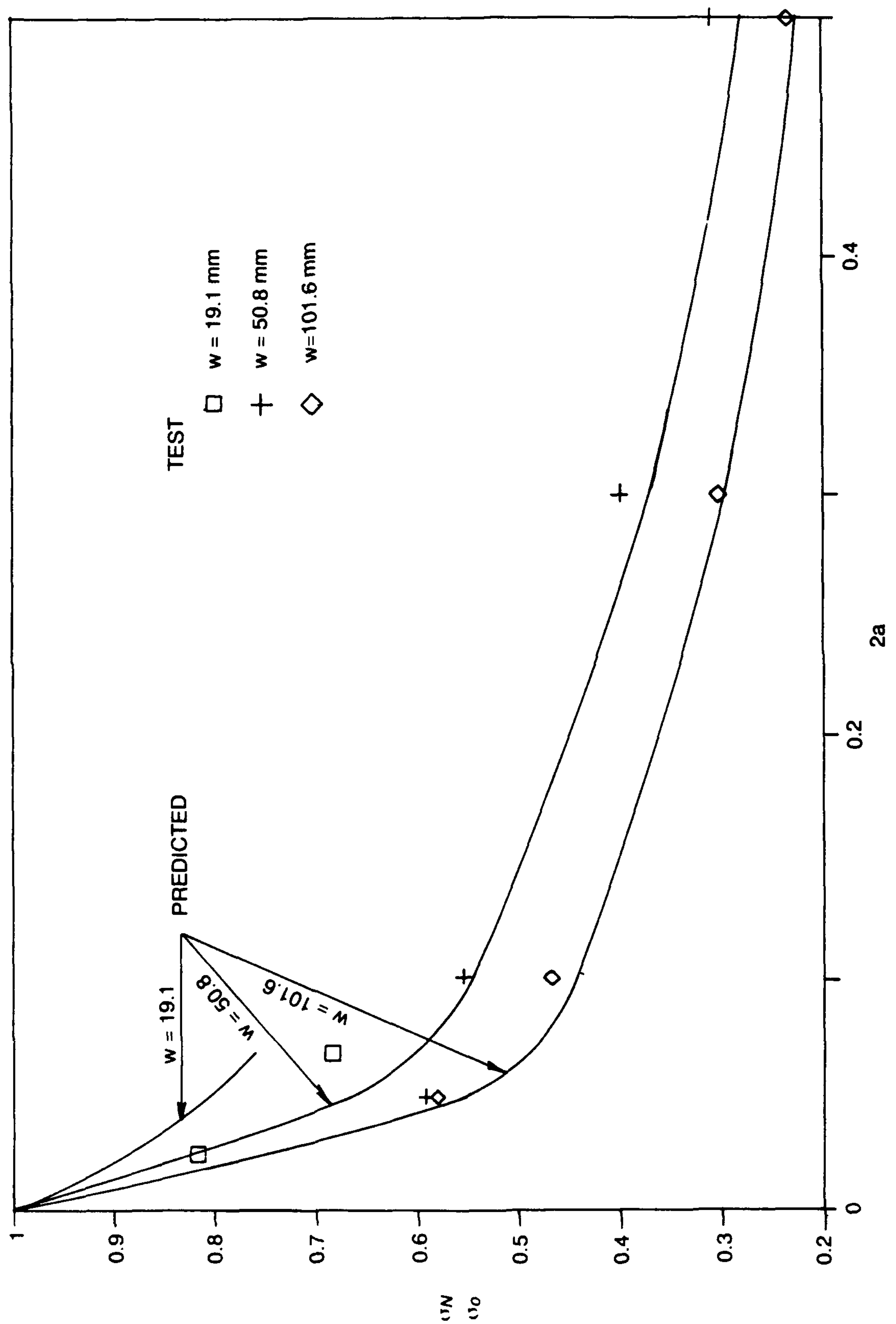

Figure 7. Comparison Of Predicted And Experimental Notched Strength Results For B/Al $(0^\circ)_{6T}$ Composites.

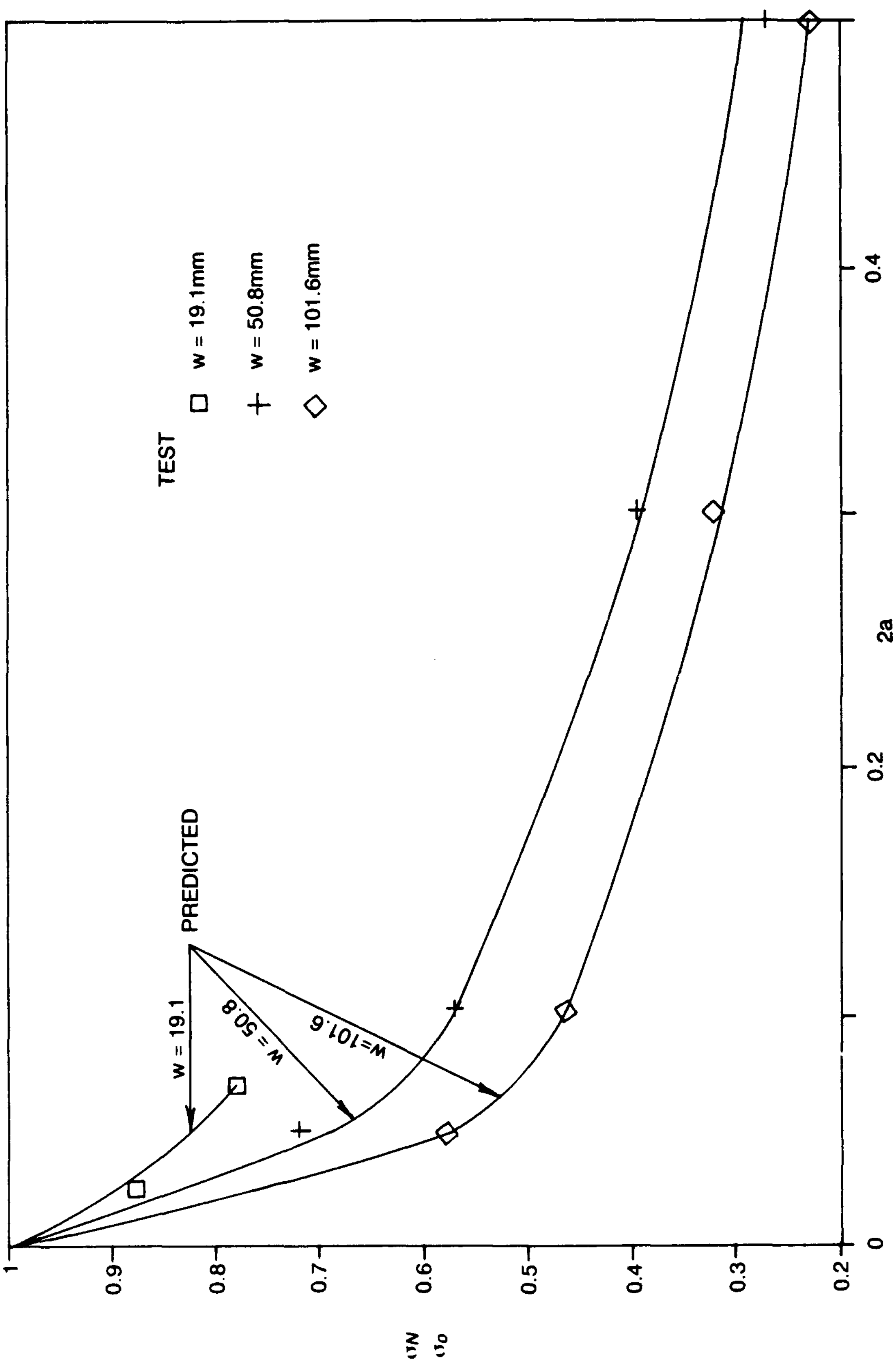

Figure 8. Comparison Of Predicted And Experimental Notched Strength Results For B/Al $[0_2/\pm45]_s$ Composites.

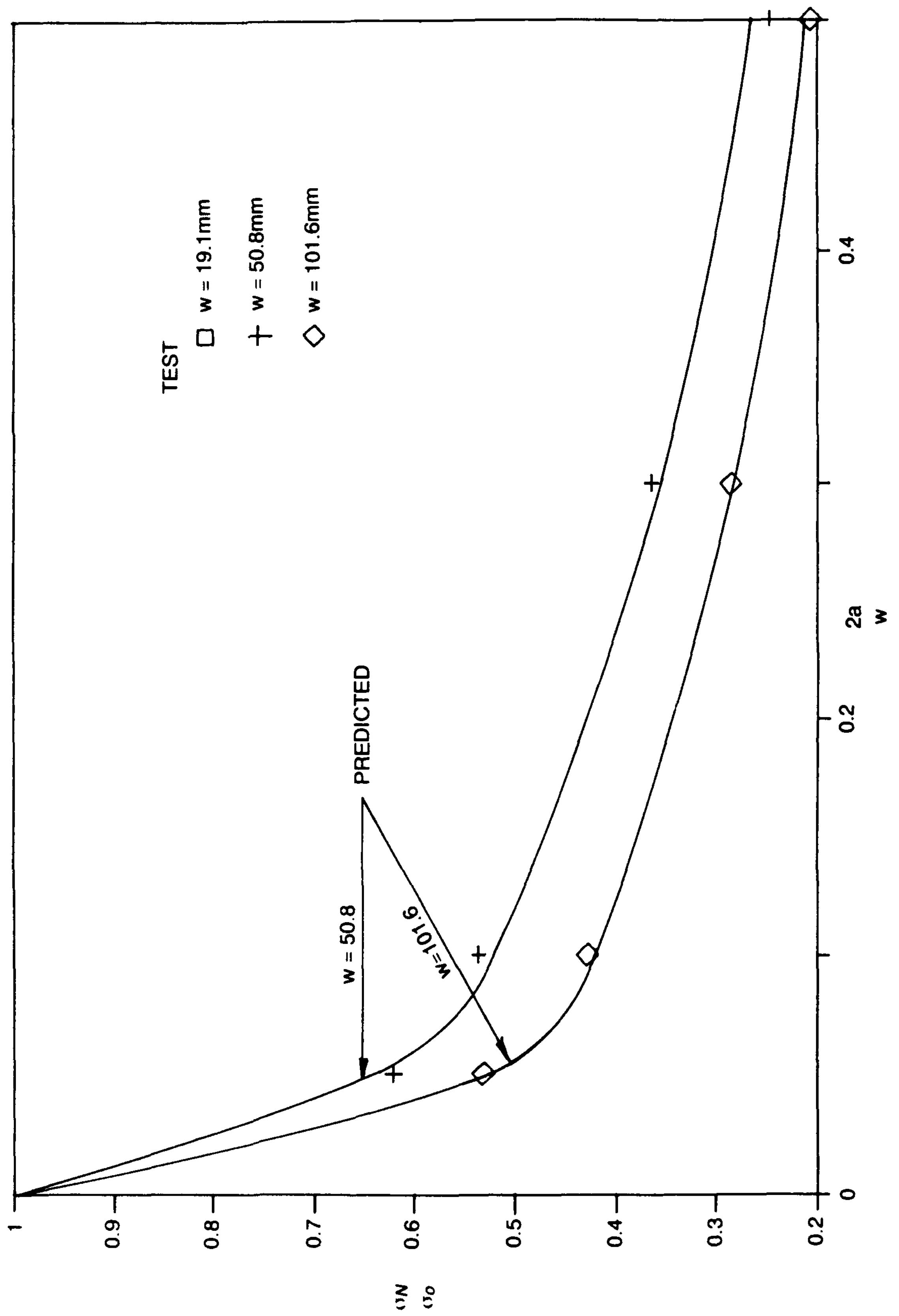

Figure 9. Comparison Of Predicted And Experimental Notched Strength Results For B/Al [±45/0$_2$]s Composites.

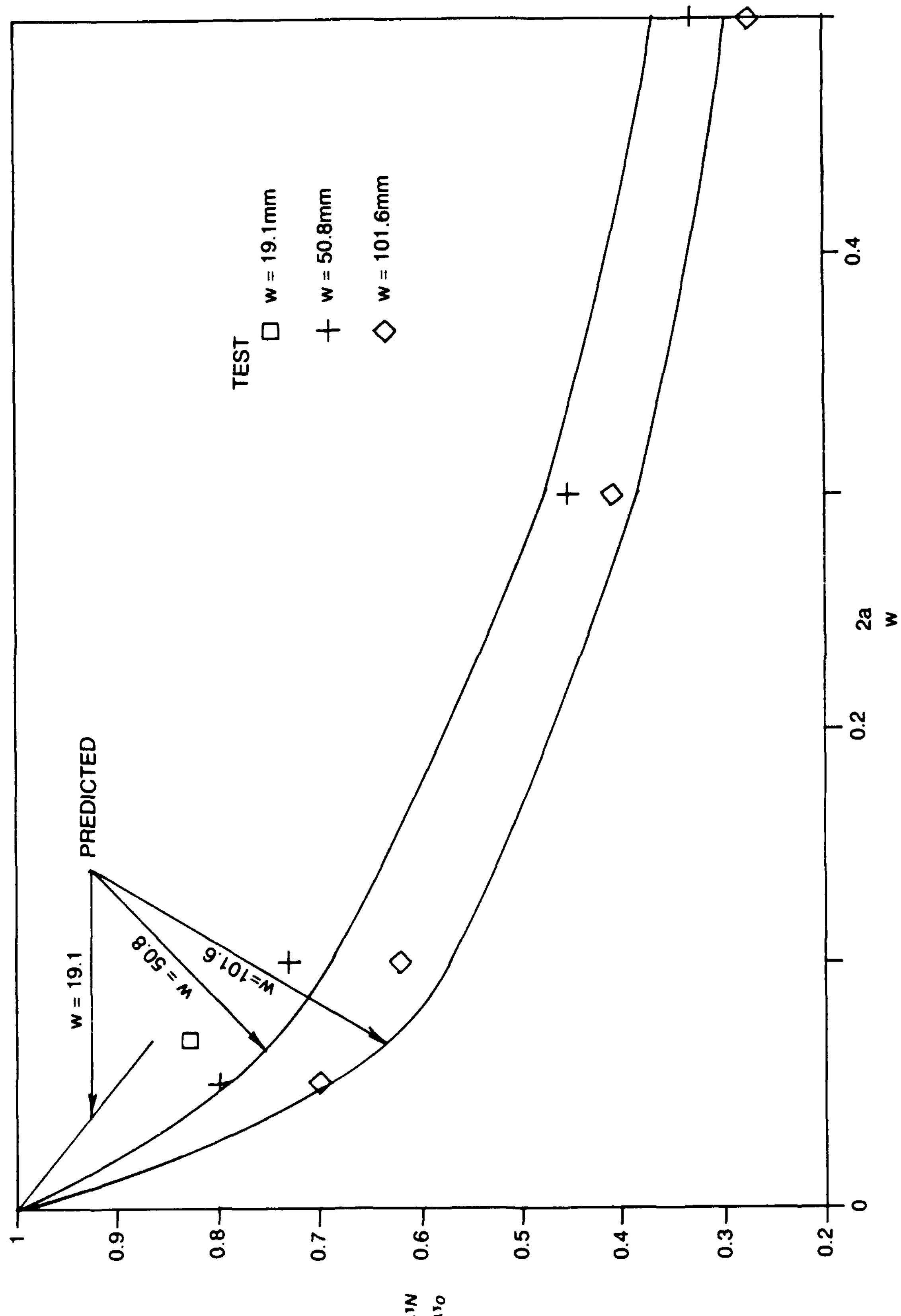

Figure 10. Comparison Of Predicted And Experimental Notched Strength Results For B/Al $[0/\pm45]_s$ Composites.

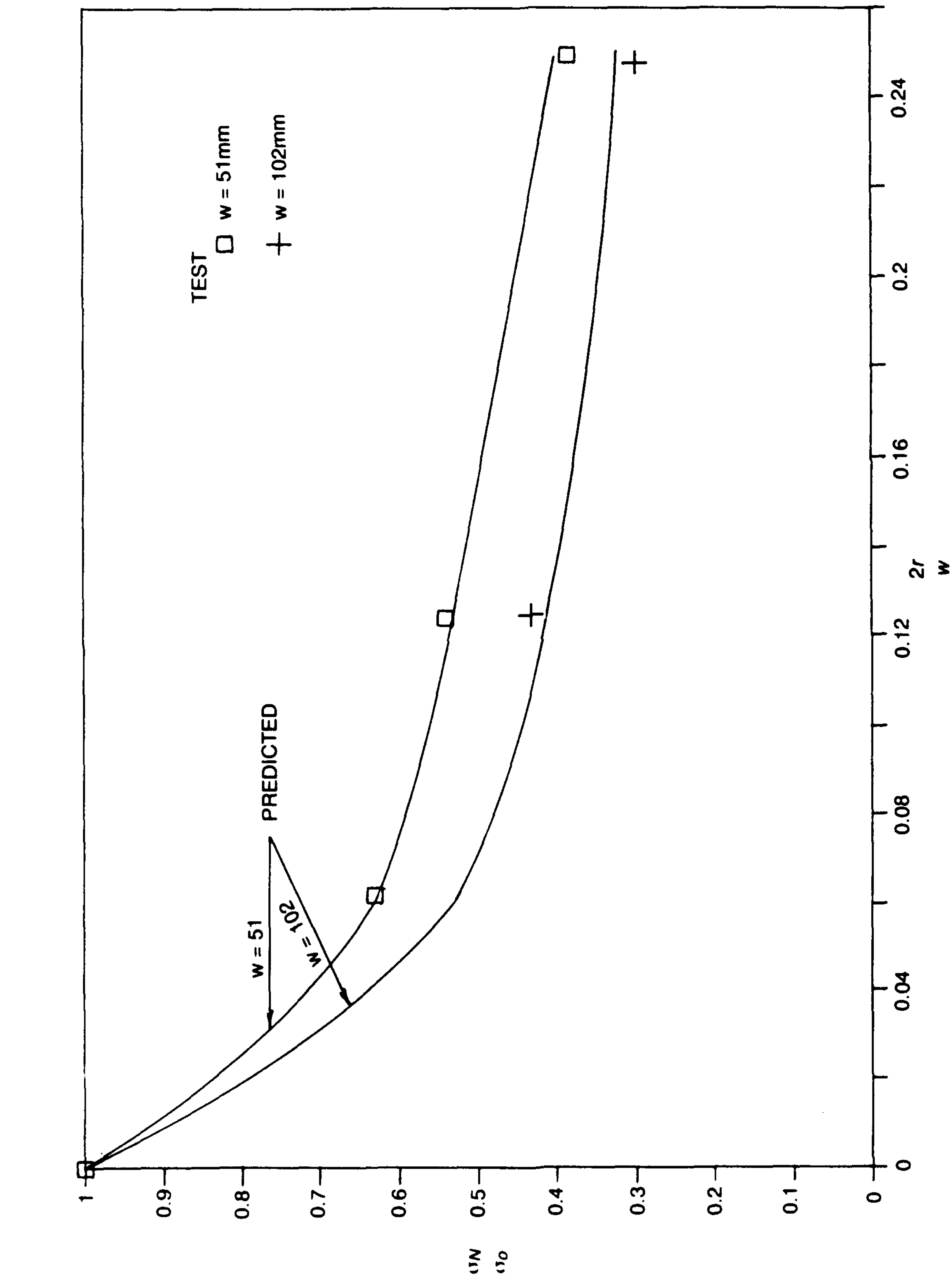

Figure 11. Notched Strength Prediction For B//Al $[0]_{6T}$ Composite With Center Hole.

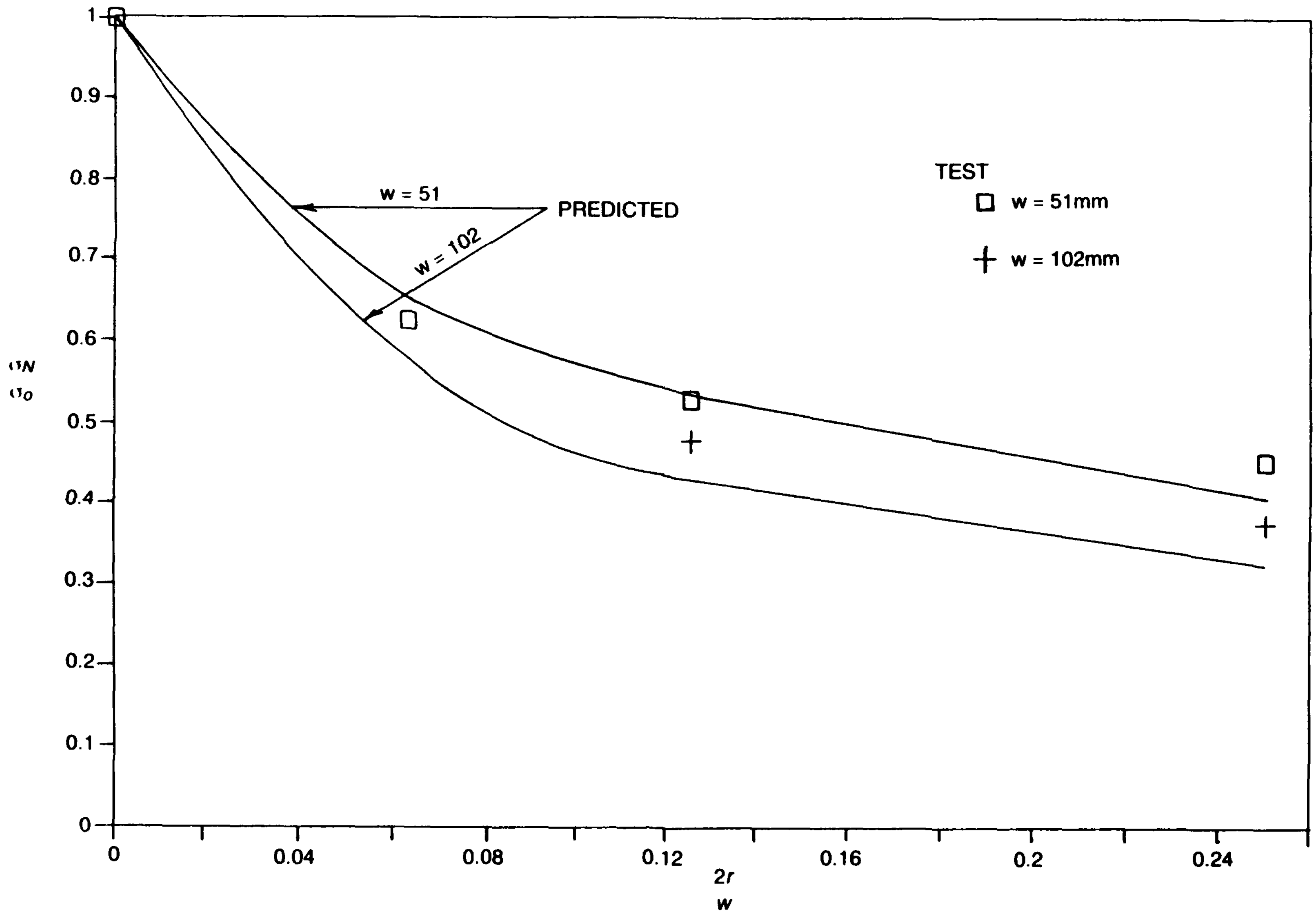

Figure 12. Notched Strength Prediction for B/Al $[0_2/\pm45]_s$ Composites With Center Hole.

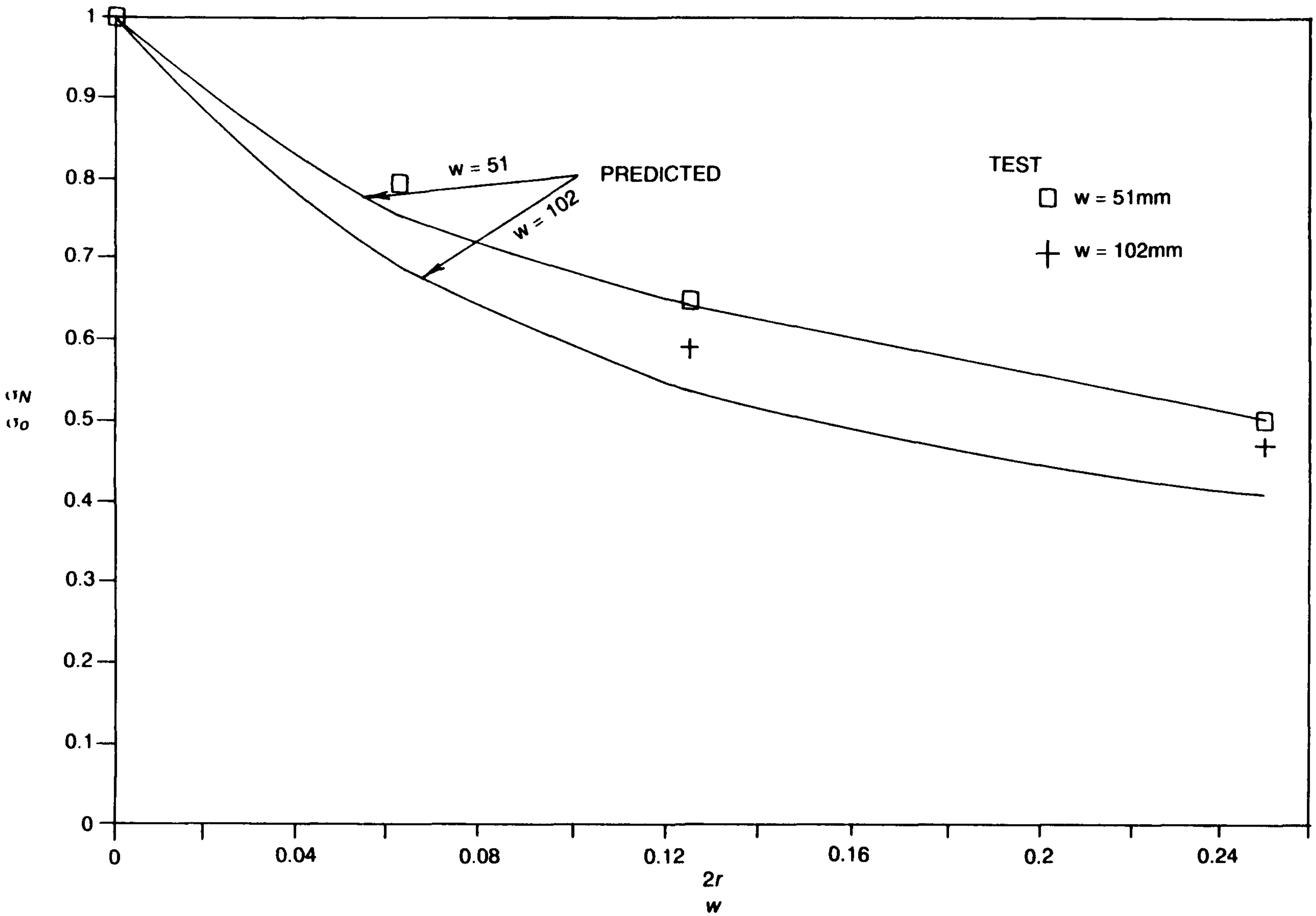

Figure 13. Notched Strength Prediction For B/Al $[0/\pm45]_s$ Composite With Center Hole.

4.1.2. Notch Sensitivity of Boron/Aluminum (B/Al) Composite Laminate

The $\frac{\sigma_N}{\sigma_O}$ test data in Tables 1 to 4 are plotted on Figures 14 to 16 for composite laminate of various widths to check the notch sensitivity of B/Al composites. It is obvious that $[\pm45/0_2]_s$ is the most notch-sensitive, while $[0/\pm45]_s$ is the least sensitive to the notch size. For $\frac{2a_o}{w} \leq .1$, $[0]_{6T}$ is more sensitive to the notch size than $[0_2/\pm45]_s$. For $\frac{2a_o}{w} > .1$, the $\frac{\sigma_N}{\sigma_O}$ vs $\frac{2a_o}{w}$ curve for $[0]_{6T}$ and $[0_2/\pm45]_s$ laminates are almost identical. The trend mentioned above can be detected by using a parameter[15] defined by the ratio $\frac{\bar{K}_Q}{\sigma_O}$ as shown in Table 7. The ranking of various laminate configurations for the $\frac{\bar{K}_Q}{\sigma_O}$ index is $[0/\pm45]_s$, $[0_2/\pm45]_s$, $[0]_{6T}$ and $[\pm45/0_2]_s$ in descending order. The relative values of $\frac{\bar{K}_Q}{\sigma_O}$ show a similar trend to that of damage zone size, C_O.

It can be concluded that the larger the ratio $\frac{\bar{K}_Q}{\sigma_O}$ (or the damage zone size C_O) the less fracture sensitivity there is to the notch size.

4.2 GRAPHITE/EPOXY (Gr/Ep) COMPOSITE

Equation (9) is used to characterize the $\bar{K}_Q$ for Gr/Ep composites.[6] The detailed calculations are shown in Appendix B.2. $\bar{K}_Q$ for various ply orientations is plotted as shown in Figures 17 to 19. It can be seen that $\bar{K}_Q$ for Gr/Ep composites can be treated as a material constant. Table 8 summarizes the characterization results of Gr/Ep composite laminates. For Gr/Ep, m = .297.

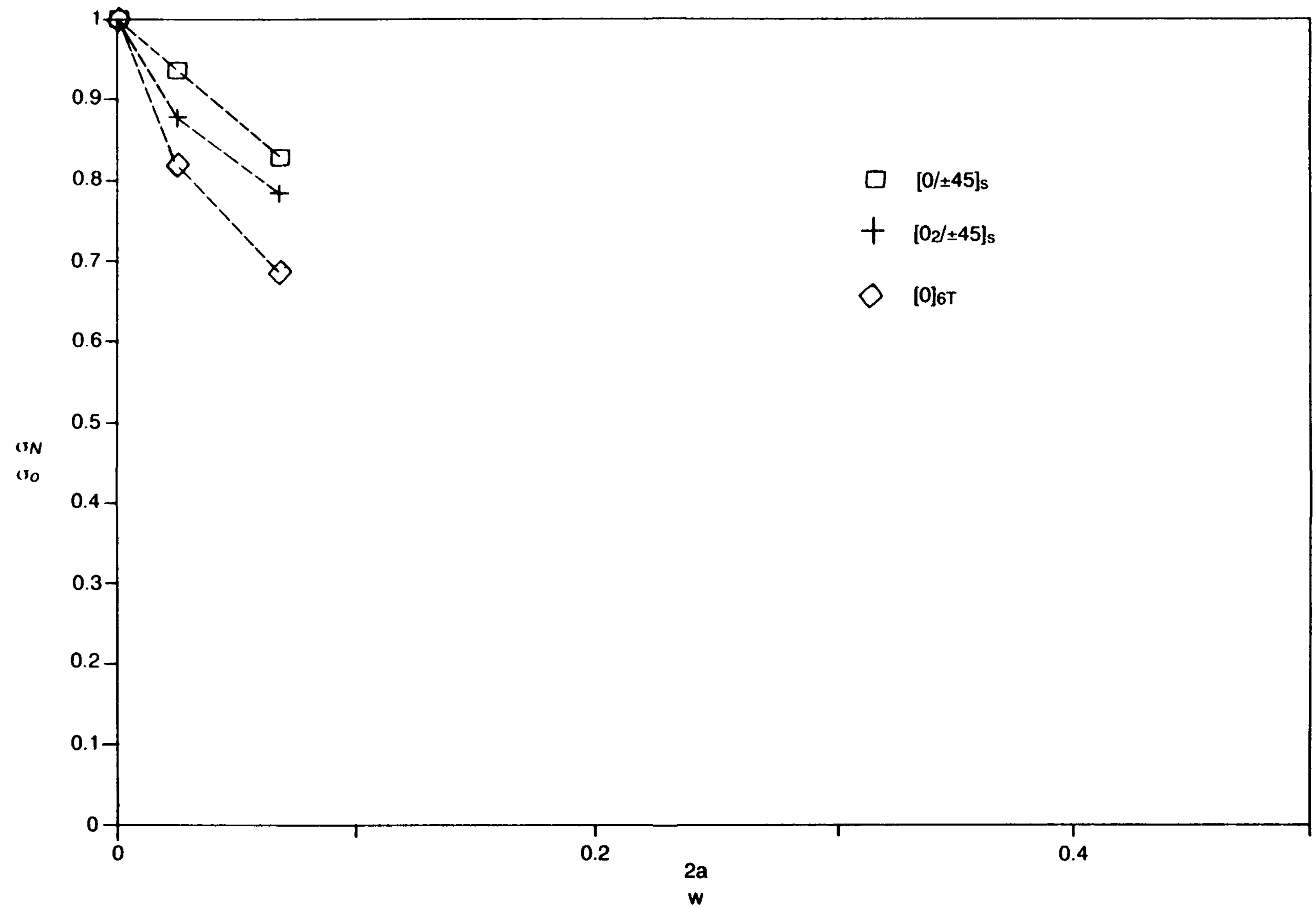

Figure 14. Notch Sensitivities For Various B/Al Laminate Orientations (w = 19.1mm).

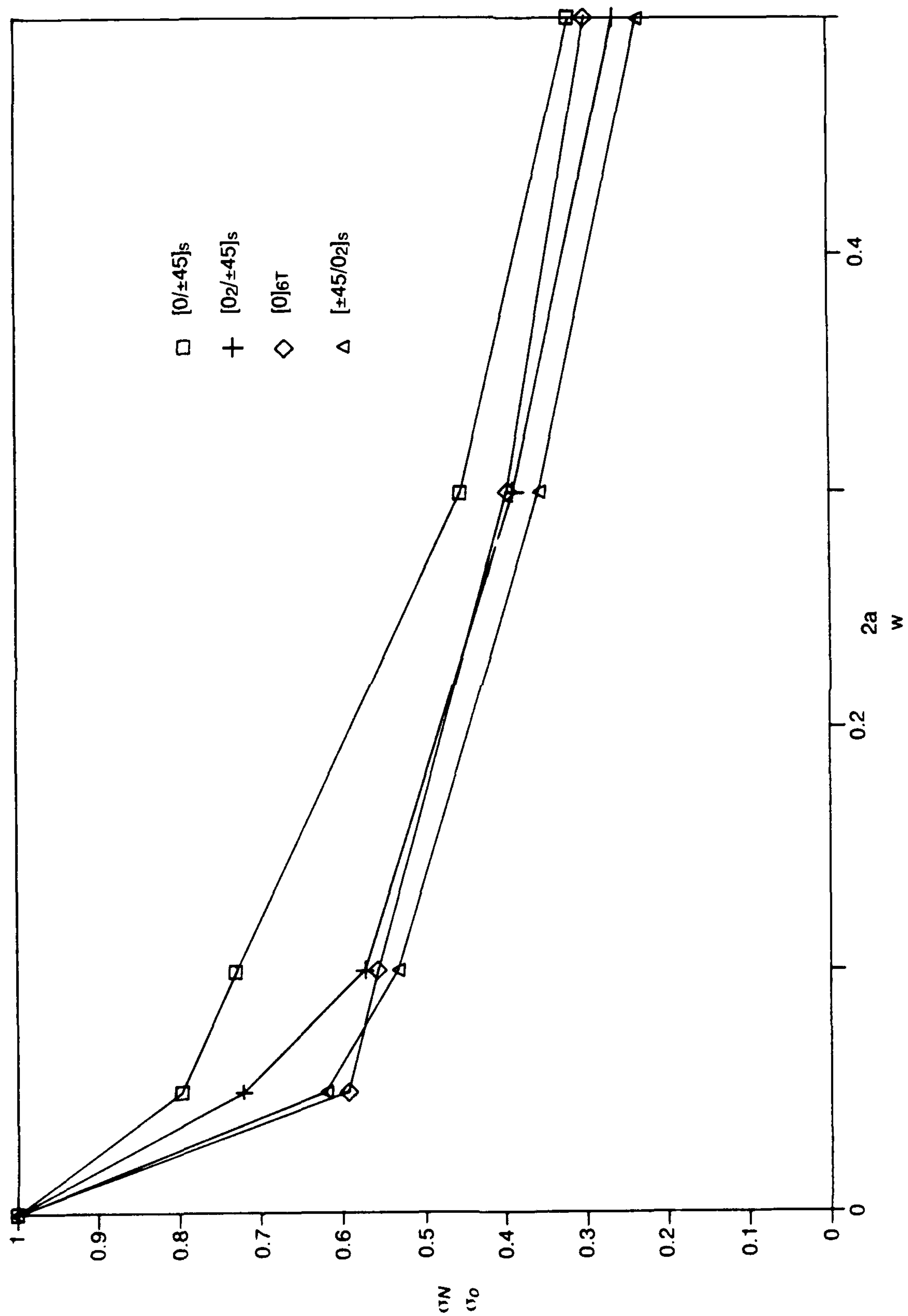

Figure 15. Notch Sensitivities For Various B/Al Laminate Orientations (w = 50.8mm).

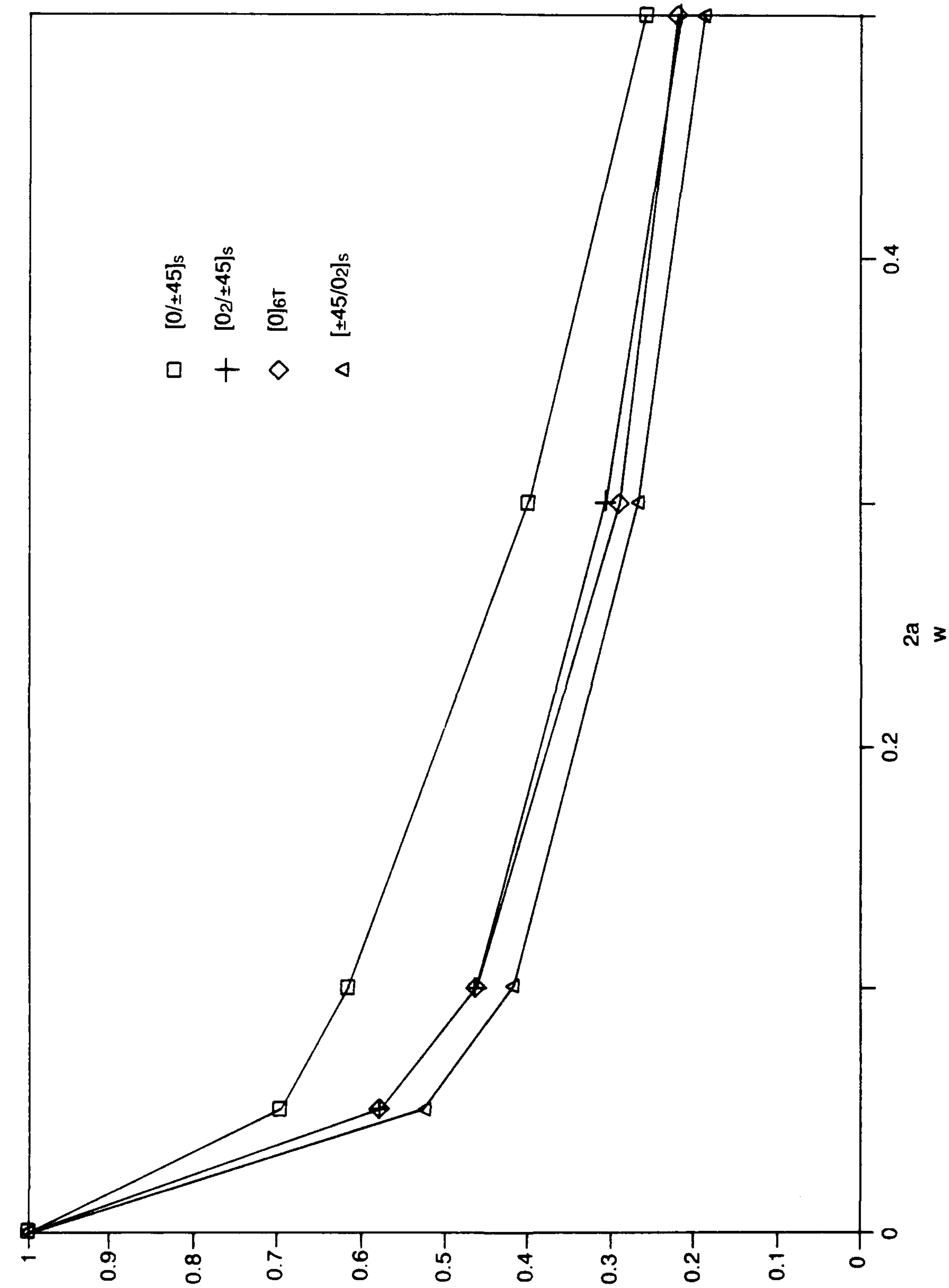

Figure 16. Notch Sensitivities For Various B/Al Laminate Orientations (w = 101.6mm).

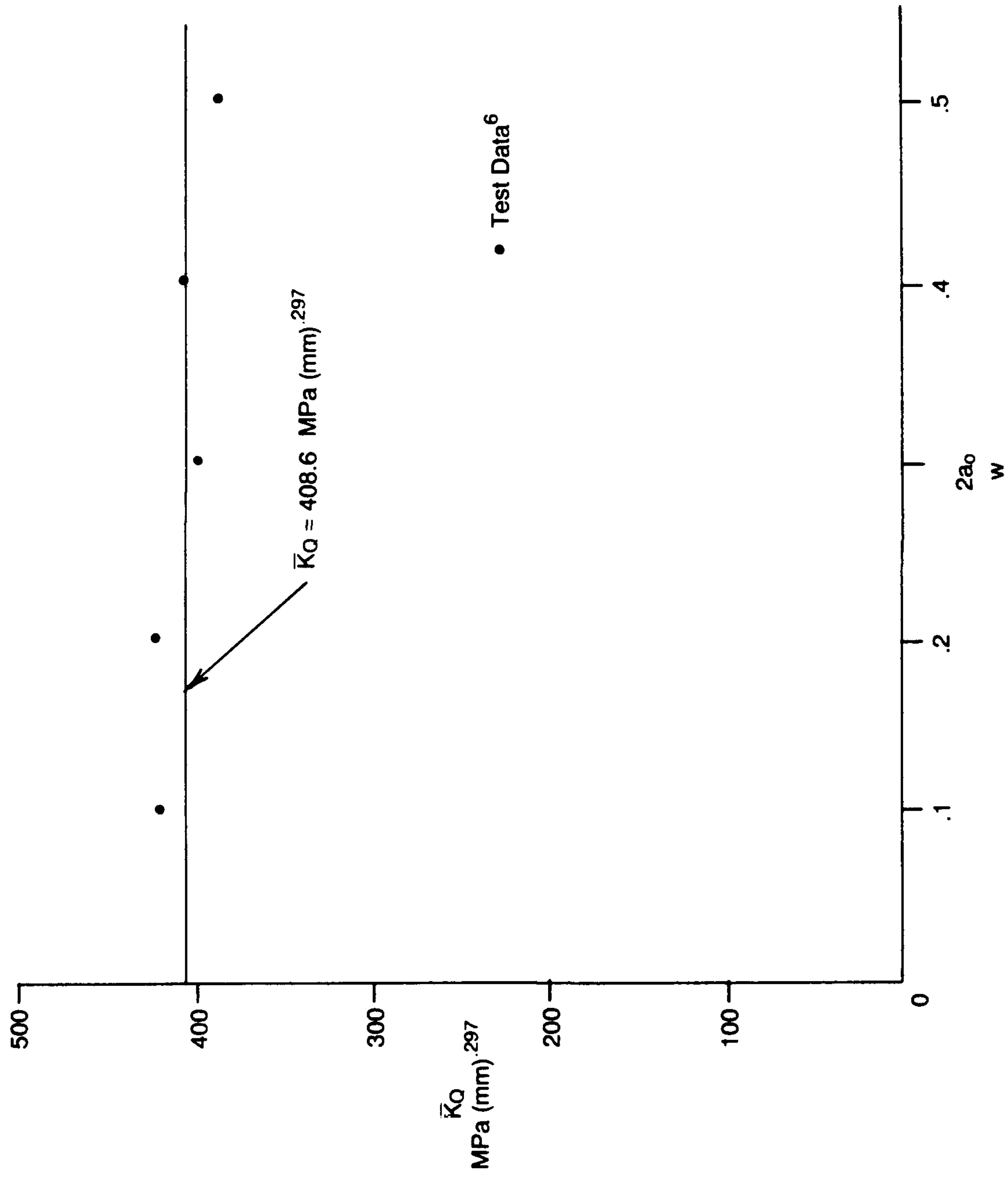

Figure 17. $\bar{K}_Q$ For Gr/Ep With Ply Orientation $[0/\pm45]_{2S}$.

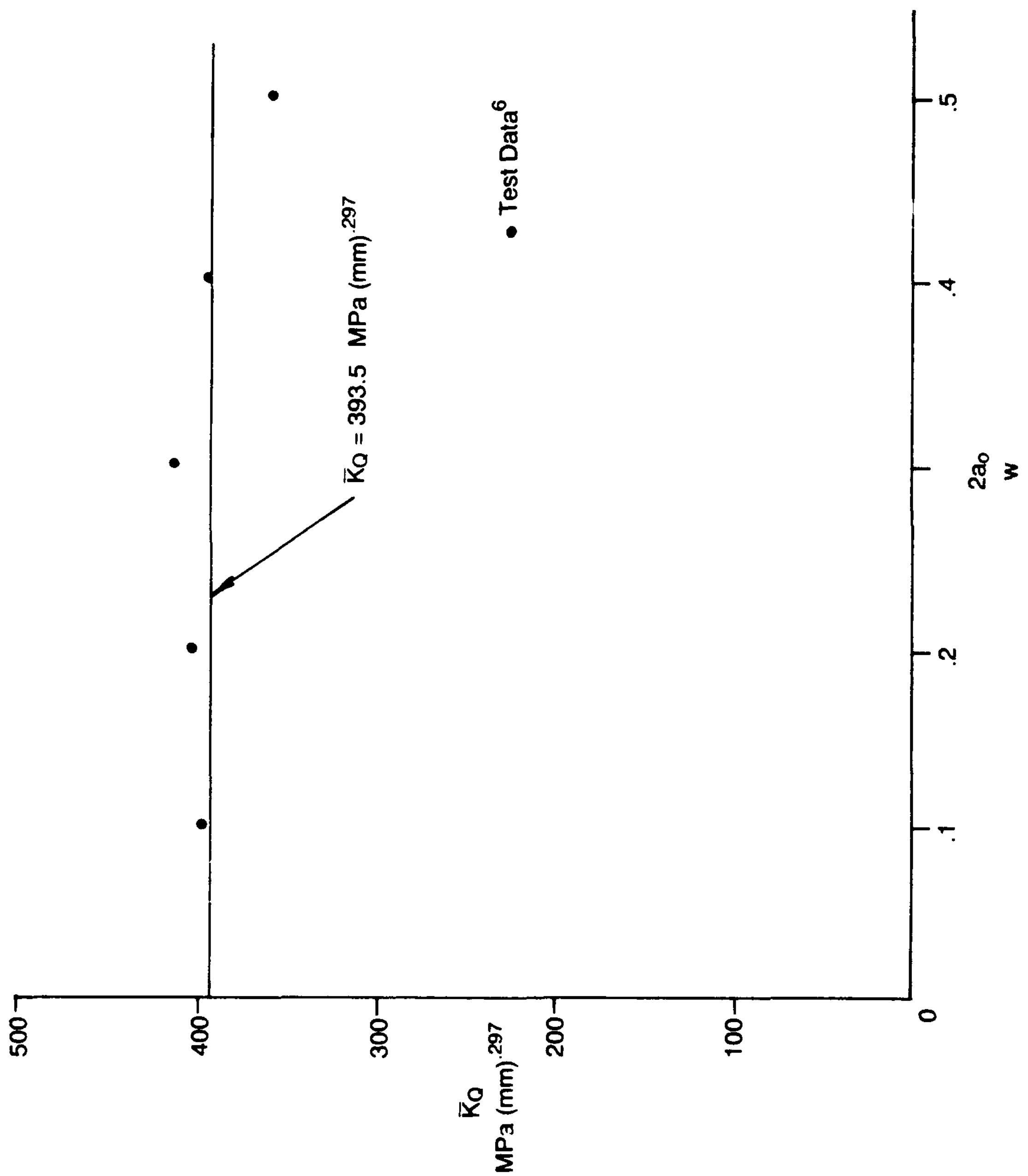

Figure 18. $\bar{K}_Q$ for Gr/Gp With Ply Orientation $[0/\pm45]_S$.

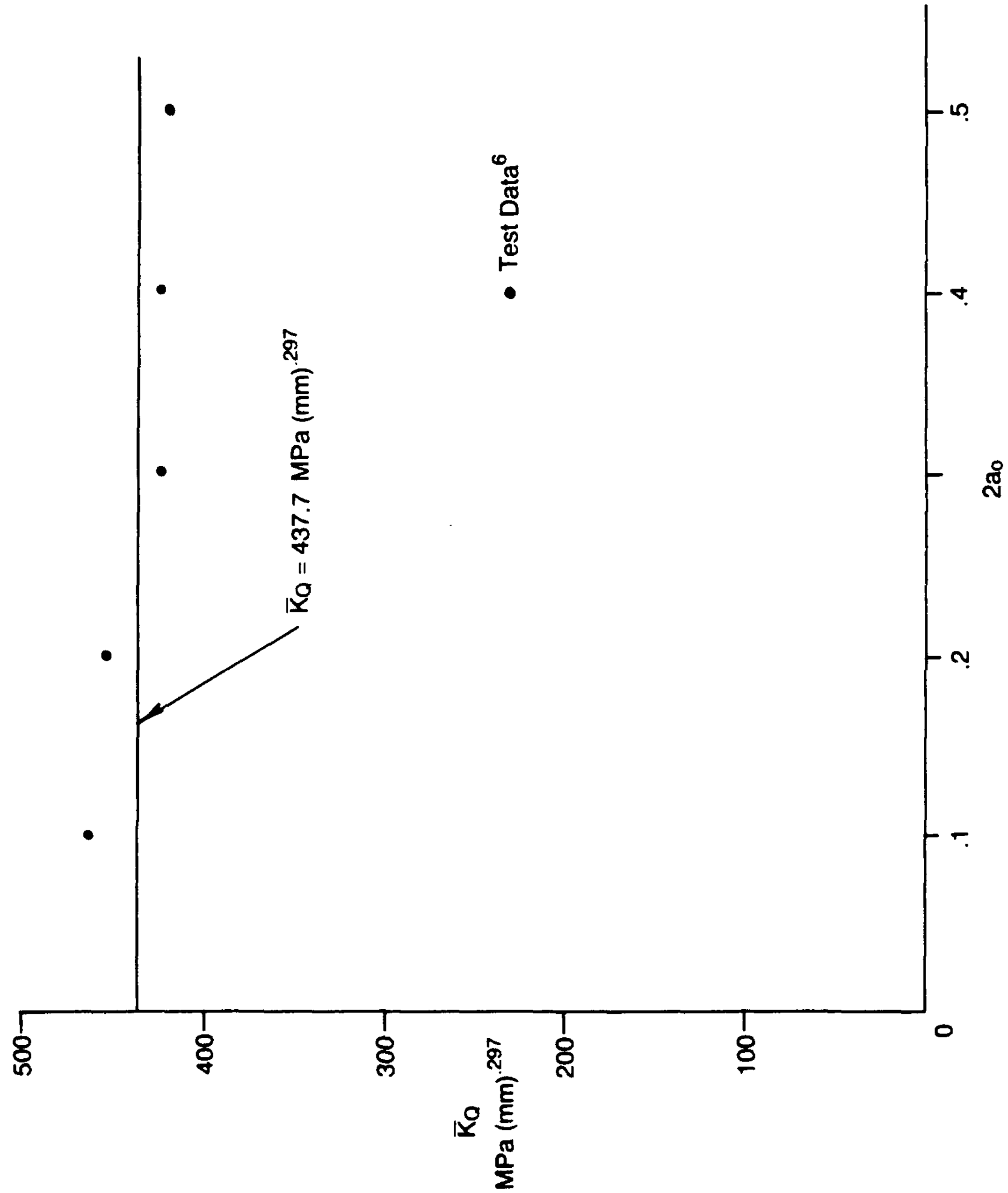

Figure 19. $\bar{K}_Q$ For Gr/Ep With Ply Orientation $[0/90/\pm45]_s$.

4.2.1 Notched Strength Prediction and Notch Sensitivity

For Gr/Ep composite with center crack, equation (17) becomes

$$\frac{\sigma_N}{\sigma_o} = \frac{1}{Y}\left\{1 + \left(\frac{\overline{K}_Q}{\sigma_o}\right)^{-3.367} a_o\right\}^{-.297} \tag{19}$$

Substituting $\overline{K}_Q$ and σ_o from Table 8, into equation (19), the fracture strengths of graphite/epoxy for various ply orientations can be obtained and are plotted on Figure 20. The detailed calculations are shown in Appendix B.2. As can be seen from the figure, the correlation between analytical and experimental results is very good.

It can also be seen from Figure 20 that the ratio $\frac{\overline{K}_Q}{\sigma_o}$ (or the inherent flaw size) in Table 8 can be used as a notch sensitivity indicator. The $[0/90/\pm45]_s$ laminate is less notch sensitive than the $[0/\pm45]_s$ and $[0/\pm45]_{2s}$ laminates and accordingly it has a larger ratio of $\frac{\overline{K}_Q}{\sigma_o}$ (or C_o) than the other two laminates.

Table 8. Fracture Parameters For Various Laminate Configurations Of Gr/Ep.

Ply Configuration	σ_o (MPa)	$\bar{K}_Q$ MPa (mm)$^{.297}$	$\frac{\bar{K}_Q}{\sigma_o}$ (mm)$^{.297}$	C_o (mm)
$[0/\pm45]_{2s}$	541.0	408.6	.755	.389
$[0/\pm45]_s$	541.0	393.5	.727	.342
$[0/90/\pm45]_s$	454.0	437.7	.964	.884

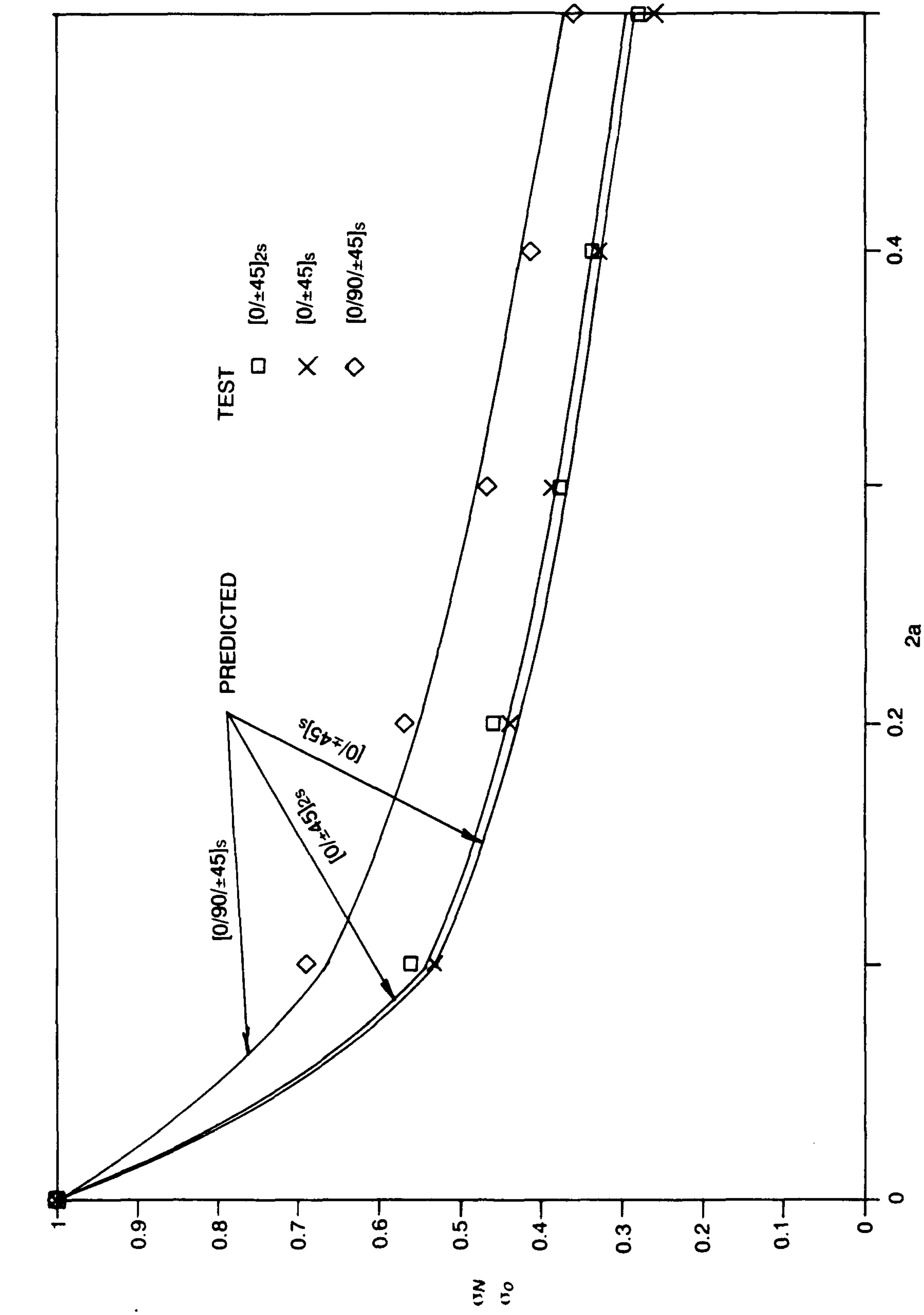

Figure 20. Notch Strength And Notch Sensitivities For Various Gr/Ep Laminate Orientations.

4.3 GLASS/EPOXY (Gl/Ep) COMPOSITE

Equation (9) is also used to characterize the $\overline{K}_Q$ for glass/epoxy composites.[16] The detailed calculations are shown in Appendix B.3. $\overline{K}_Q$ for $[0/\pm 45/90]_{2S}$ ply orientation is plotted against $\frac{2a}{w}$ in Figure 21. For Gl/Ep composite m = .289. As seen in the figure, $\overline{K}_Q$ can be approximately treated as a material constant.

For Gl/Ep composites with center crack, equation (17) becomes

$$\frac{\sigma_N}{\sigma_O} = \frac{1}{Y}\left\{1 + \left(\frac{\overline{K}_Q}{\sigma_O}\right)^{-3.46} a_O\right\}^{-.289} \qquad (20)$$

with

$$\overline{K}_Q = 274 \text{ MPa (mm)}^{.289}$$

$$\sigma_O = 320 \text{ MPa}$$

Equation (20) becomes

$$\frac{\sigma_N}{\sigma_O} = \frac{1}{Y}\{1 + 1.7108\, a_O\}^{-.289} \qquad (21)$$

For the laminate with a center crack[8],

$$Y = \sqrt{\sec\left(\frac{\pi a_O}{w}\right)} \qquad (22)$$

where a_O = half crack length.

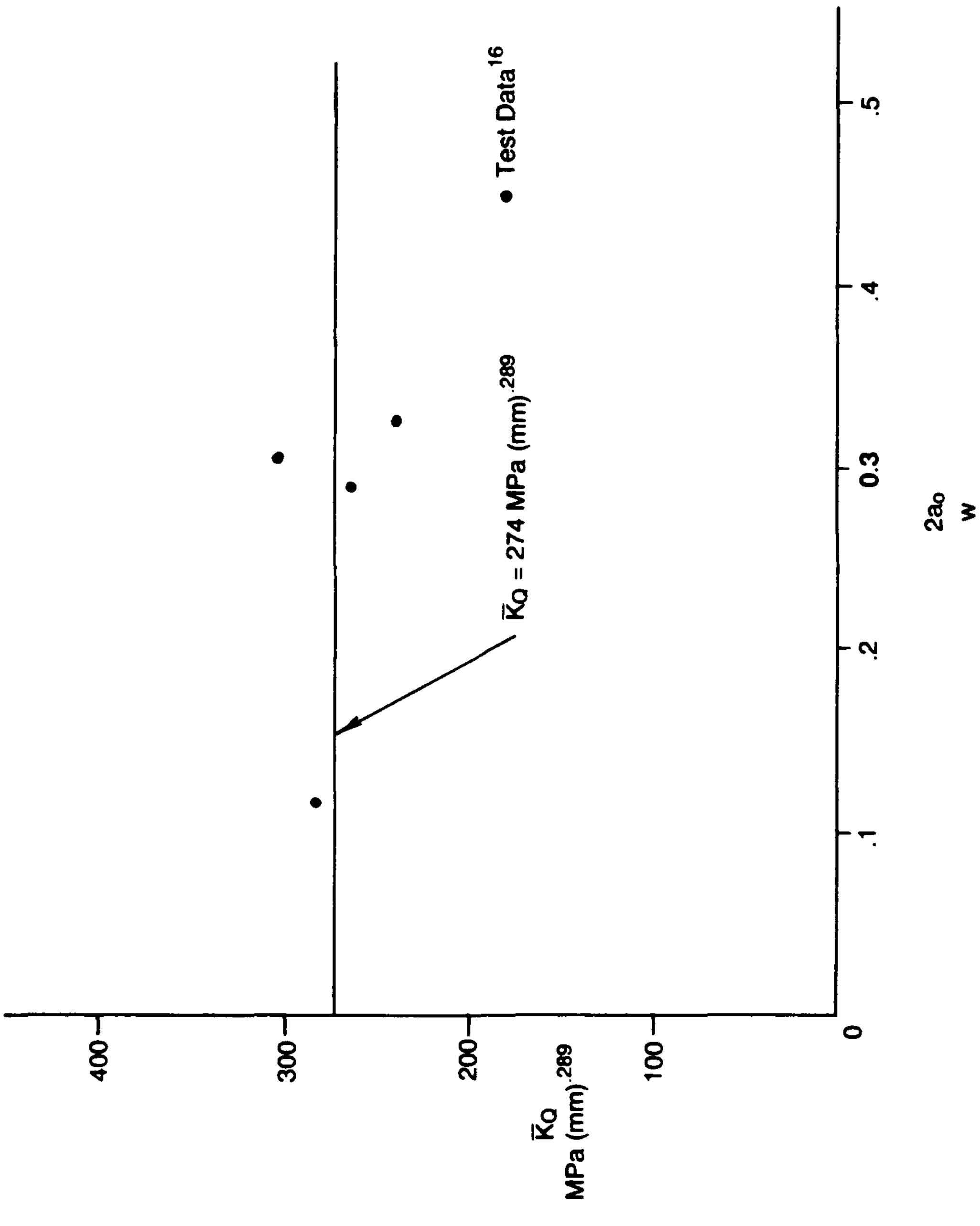

Figure 21. $\overline{K}_Q$ for Gl/Ep with Ply Orientation $[0/\pm45/90]_{2s}$.

For the laminate with a center hole. Y is assumed in the following form

$$Y = \sqrt{\sec\left(\frac{\pi R_o}{w}\right)} \tag{23}$$

where R_o = radius of the hole

Equation (21) was plotted for Gl/Ep $[0/\pm 45/90]_{2s}$ laminates with a center crack and a hole as shown in Figure 22.

It can be seen that the correlations between analytical results and test results are good. Also, note that a center hole decreases the fracture strength of a composite laminate slightly more than a center crack does.

4.4 COMPARISON OF ANALYTICAL RESULTS BETWEEN ANISOTROPIC AND MICROSCOPIC MODELS

Composite materials made by combining two materials with different elastic modulii are by nature anisotropic in the gross sense. The anisotropic model for composite materials is to assume that the composite is a homogeneous, anisotropic solid. For an anisotropic fracture m = .5.[17] Applying the inherent flaw concept for an anisotropic model, for center crack specimen, we have

$$K_Q = Y\sigma_N\left(a_o + C_o^*\right)^{1/2} \tag{24}$$

$$K_Q = \sigma_o\left(C_o^*\right)^{1/2} \tag{25}$$

Note that K_Q has dimensions different from those of $\bar{K}_Q$ and C_o^* is the inherent flaw size corresponding to an anisotropic model.

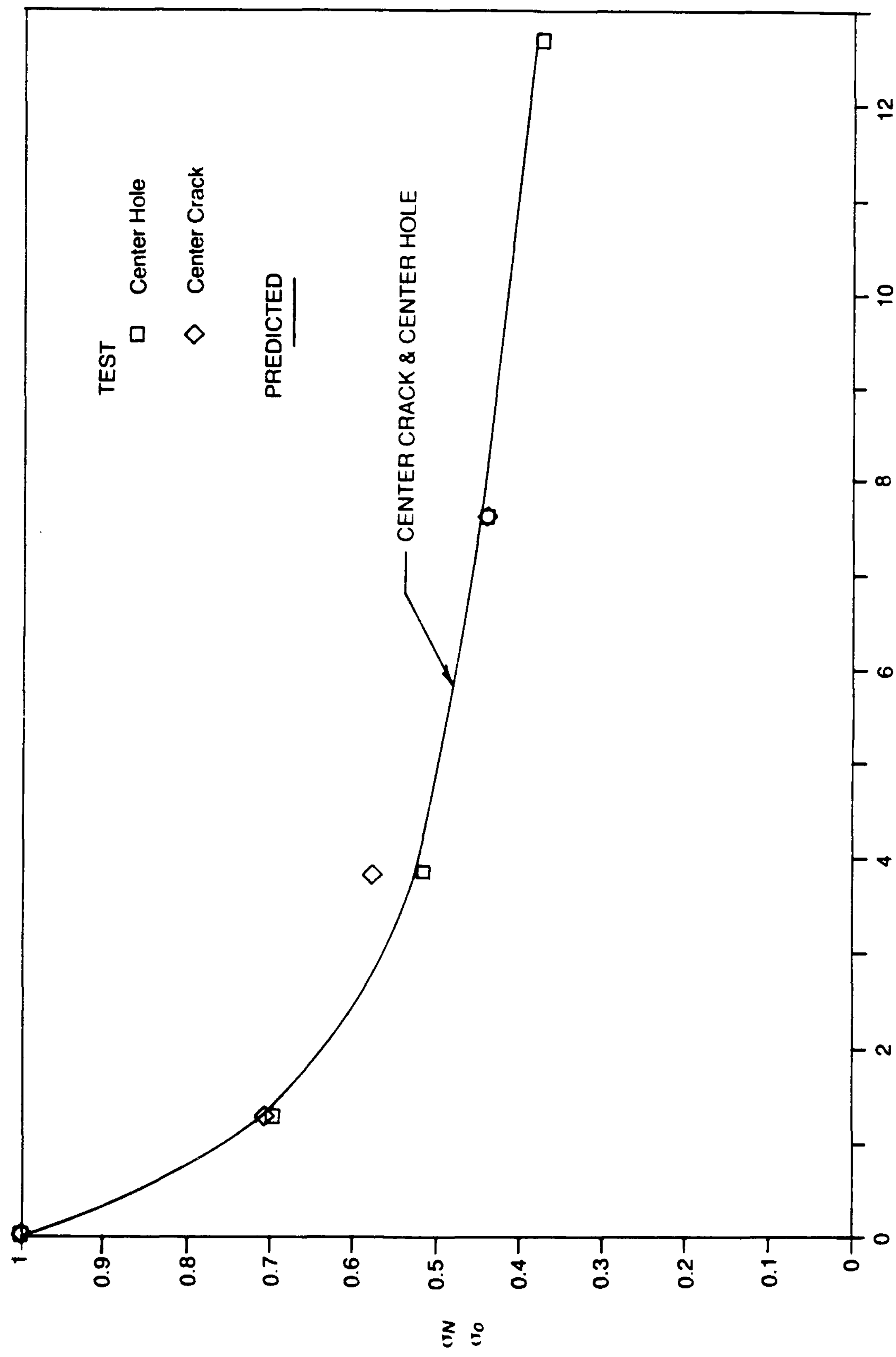

Figure 22. Fracture Strength Prediction For Gl/Ep $[0/\pm45/90]_{2s}$.

Examining equations (24) and (25), we can derive the following useful equations for an anisotropic model

$$C_o^* = \frac{a_o}{\left(\frac{\sigma_o}{Y\sigma_N}\right)^2 - 1} \tag{26}$$

$$\frac{\sigma_N}{\sigma_o} = \frac{1}{Y}\left(\frac{C_o^*}{a_o + C_o^*}\right)^{1/2} \tag{27}$$

$$K_Q = \sigma_o \left(a_o\right)^{1/2}\left\{\left(\frac{Y\sigma_N}{\sigma_o}\right)^{-2.0} - 1\right\}^{-.5} \tag{28}$$

Equation (26) can be used to obtain C_o^* through the least square fit method. It has been determined for the anisotropic model that C_o^* found by the least square fit method predicts the test data better than C_o^* found by the average equivalent stress intensity method. Equation (27) can be used to predict the fracture strength of composite laminates.

In this report, only B/Al composites will be used to demonstrate the superiority of the microscopic model over the anisotropic model.

Tables 9 to 12 show the comparison of analytical results between the microscopic and anisotropic models. These results are also plotted on Figures 23 to 26. It is clear that the microscopic model predicts better results than the anisotropic model. Note that the results of the *microscopic model are copied* from Tables 1 to 4, while the results of the anisotropic model are shown in Appendix C.

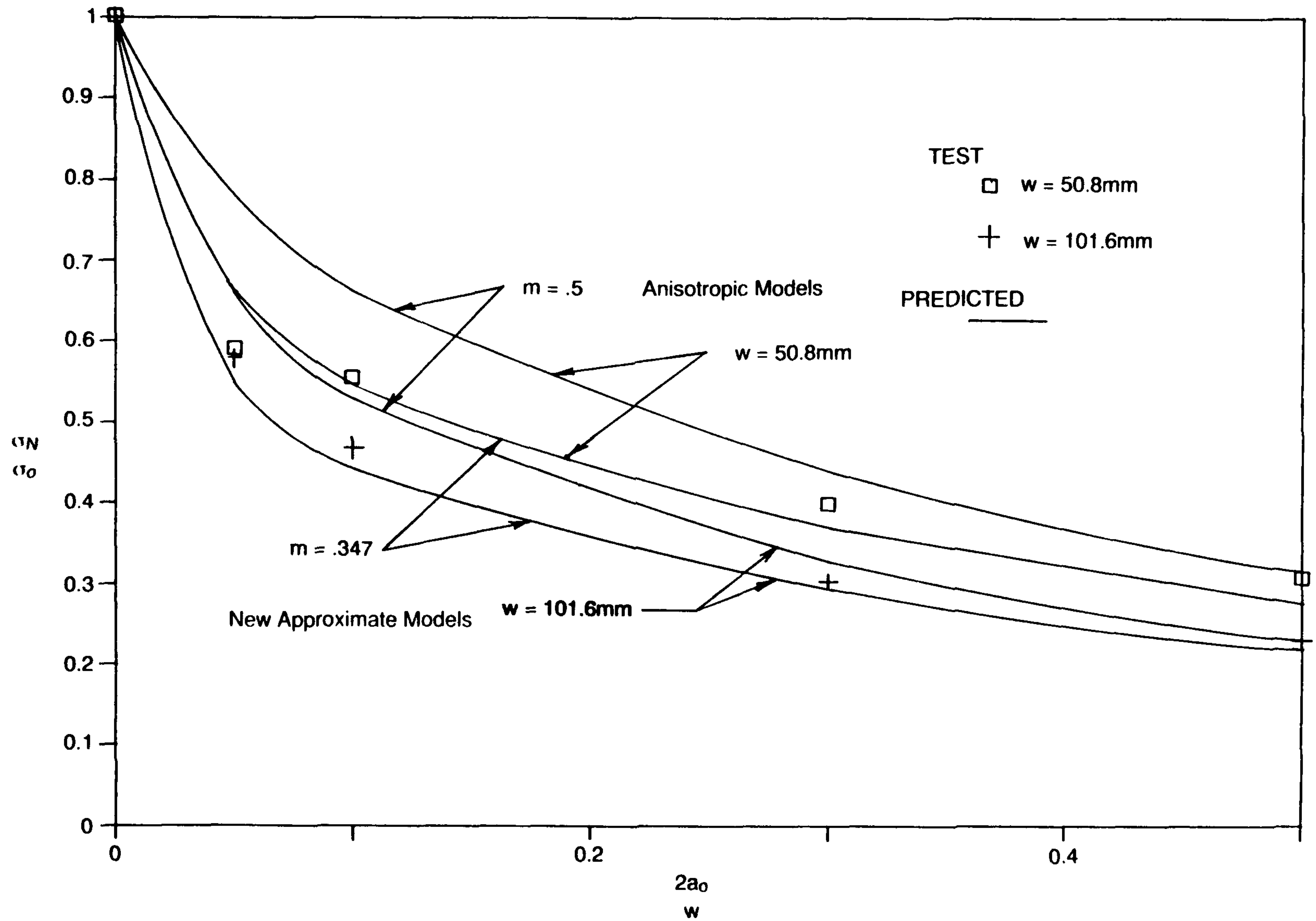

Figure 23. Comparison Of Analytical Results Between Anisotropic And New Approximate Models B/Al $(0)_{6T}$.

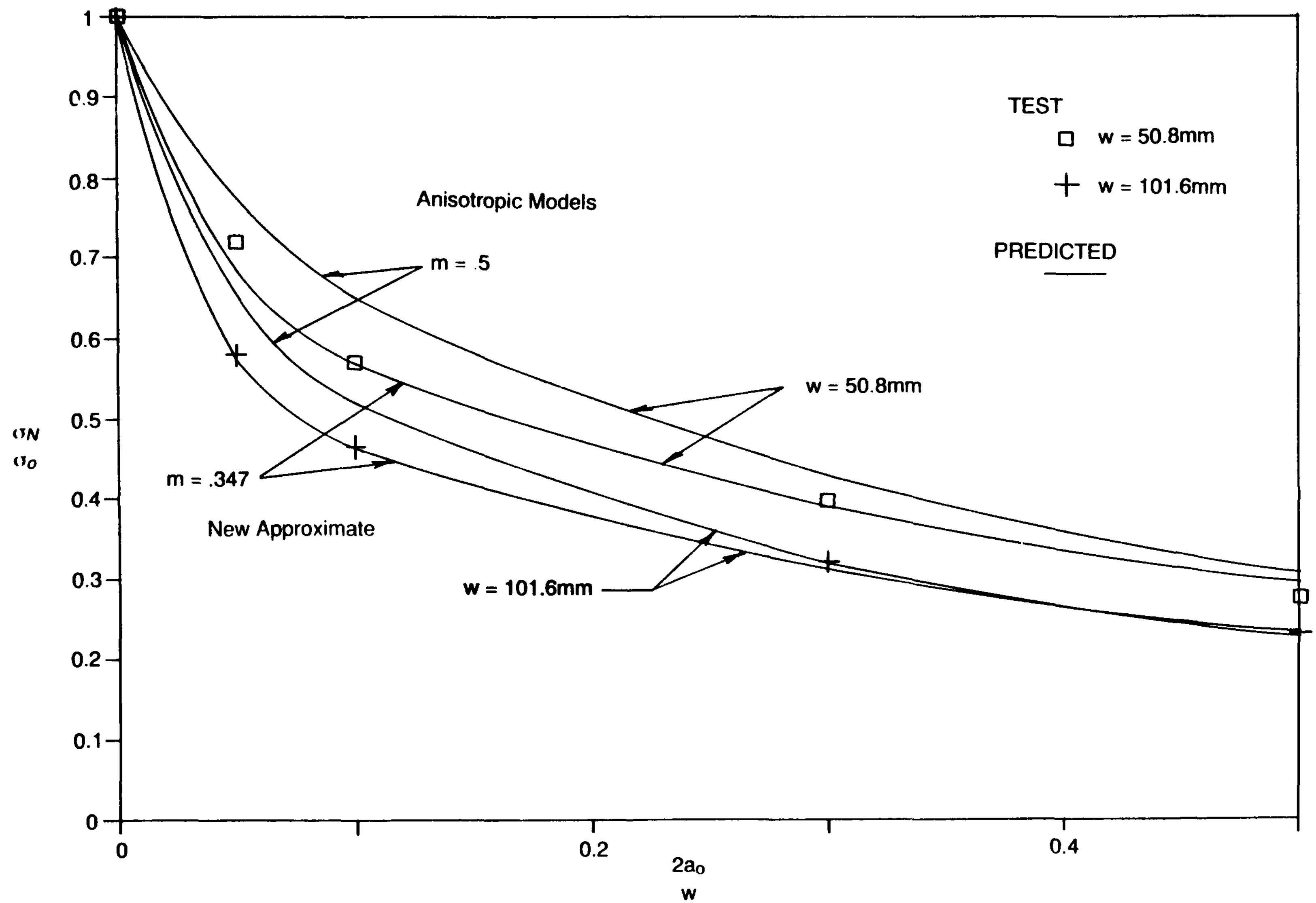

Figure 24. Comparison Of Analytical Results Between Anisotropic And New Approximate Models B/Al $(0_2/\pm45)_s$.

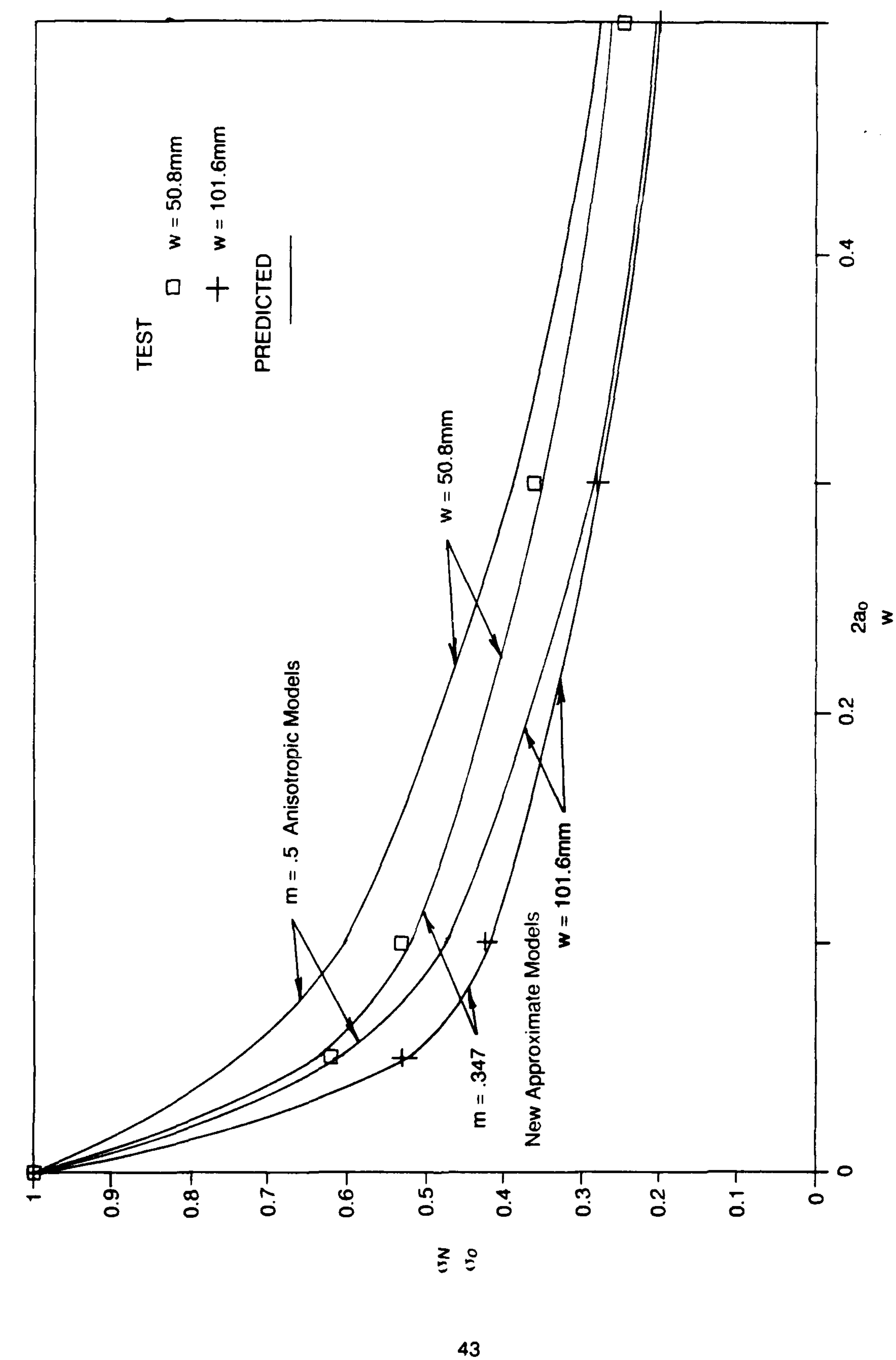

Figure 25. Comparison Of Analytical Results Between Anisotropic And New Approximate Models B/Al ($\pm 45/0_2)_S$.

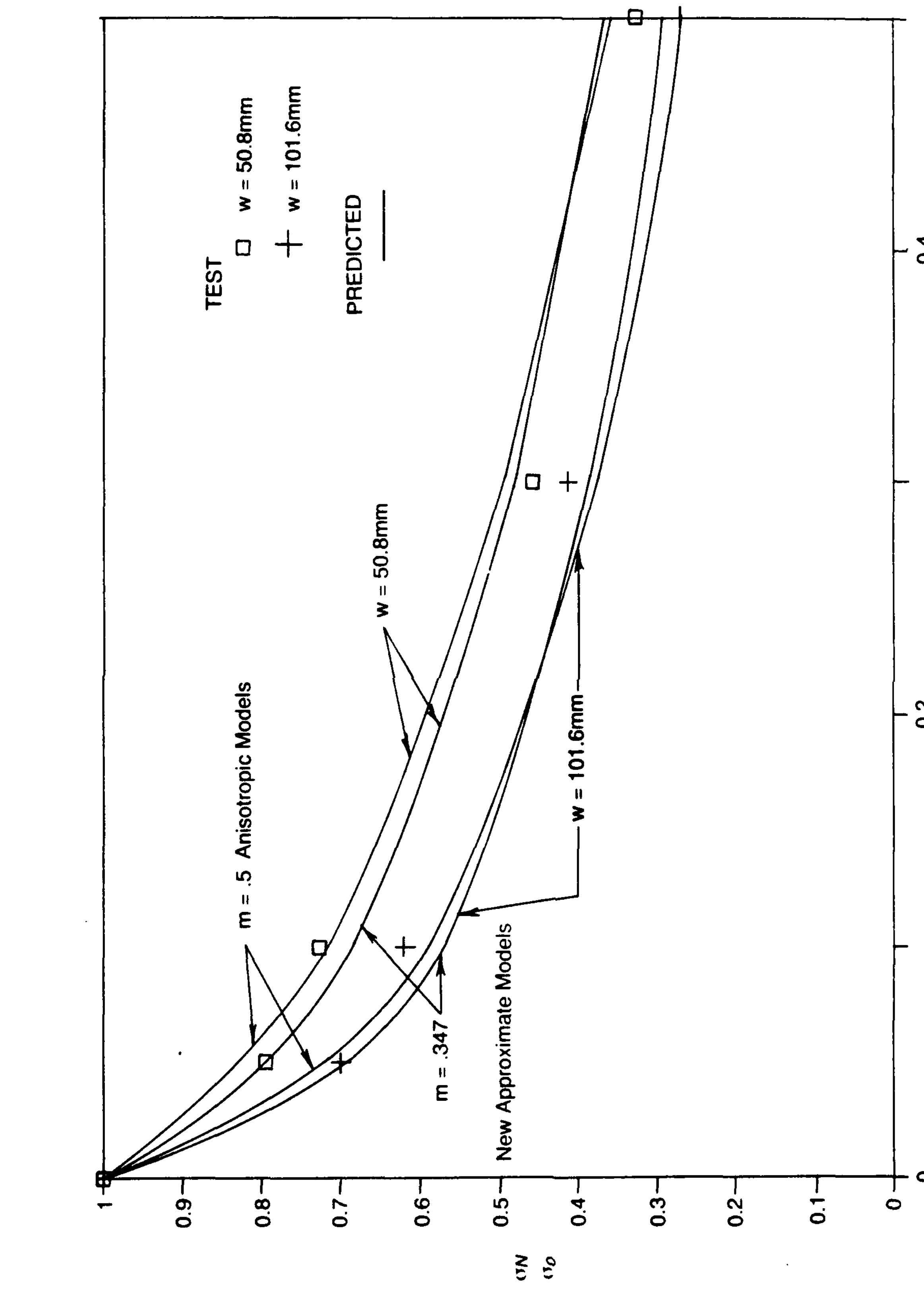

Figure 26. Comparison Of Analytical Results Between Anisotropic And New Approximate Models B/Al $(0/\pm45)_s$.

Table 9. Comparison Of Analytical Results Between Anisotropic And New Approximate Models B/Al $[0]_{6T}$.

a_o (mm)	$\frac{2a_o}{W}$	$\left(\frac{\sigma_N}{\sigma_o}\right)_{Test}$	Microscopic Model (m = .347)	Anisotropic Model (m = .5)
0.25	.03	.818	.878	.942
.65	.07	.6845	.760	.866
1.25	.05	.592	.663	.786
2.55	.05	.580	.549	.666
2.55	0.10	.555	.546	.663
5.10	0.1	.468	.443	.532
7.60	0.3	.4003	.371	.44
12.7	0.5	.3098	.279	.317
15.25	0.3	.3024	.295	.329
25.40	0.5	.232	.221	.233

Table 10. Comparison Of Analytical Results Between Anisotropic And New Approximate Models B/Al $[0_2/\pm45]_s$.

a_o (mm)	$\frac{2a_o}{W}$	$\left(\frac{\sigma_N}{\sigma_o}\right)_{Test}$	Microscopic Model (m = .347)	Anisotropic Model (m = .5)
0.25	.03	.878	.891	.938
.65	.07	.782	.782	.858
1.25	.05	.721	.686	.775
2.55	.05	.579	.572	.653
2.55	0.10	.571	.570	.649
5.10	0.1	.464	.464	.518
7.6	0.3	.395	.389	.427
12.7	0.5	.274	.293	.307
15.25	0.3	.321	.310	.318
25.40	0.5	.229	.232	.225

Table 11. Comparison Of Analytical Results Between Anisotropic And New Approximate Models B/Al $[\pm 45/0_2]_s$.

a_o (mm)	$\frac{2a_o}{w}$	$\left(\frac{\sigma_N}{\sigma_o}\right)_{Test}$	Microscopic Model (m = .347)	Anisotropic Model (m = .5)
0.25	.03	—	—	—
.65	.07	—	—	—
1.25	.05	.619	.633	.735
2.55	.05	.528	.520	.606
2.55	0.10	.531	.517	.602
5.10	0.1	.423	.417	.472
7.6	0.3	.361	.349	.386
12.7	0.5	.245	.262	.275
15.25	0.3	.281	.276	.284
25.40	0.5	.201	.207	.200

Table 12. Comparison Of Analytical Results Between Anisotropic And New Approximate Models B/Al $[0/\pm45]_s$.

a_o (mm)	$\frac{2a_o}{w}$	$\left(\frac{\sigma_N}{\sigma_o}\right)_{Test}$	Microscopic Model (m = .347)	Anisotropic Model (m = .5)
0.25	.03	—	—	—
0.65	.07	.828	.865	.895
1.25	.05	.796	.789	.828
2.55	.05	.699	.692	.721
2.55	0.10	.730	.688	.717
5.10	0.1	.620	.569	.591
7.6	0.3	.458	.481	.495
12.7	0.5	.329	.367	.361
15.25	0.3	.413	.388	.376
25.40	0.5	.271	.293	.268

5.0 CONCLUSIONS AND RECOMMENDATIONS

5.1 CONCLUSIONS

- The methodology developed here can be used to characterize the fracture toughness of the composite laminates and can be used as a design tool to predict the fracture strength of various composite laminates.

- The parameter $\overline{K}_Q$ which was called critical equivalent stress intensity factor is defined, and can be treated as a material constant for composite laminate.

- The new approximate model provides better results than those of the anisotropic model.

- The larger the ratio $\frac{\overline{K}_Q}{\sigma_o}$ (or the inherent flaw size, C_o), the higher the damge tolerance.

5.2 RECOMMENDATIONS

- Further verification of microscopic theory with test results of various composites materials is needed.

- Apply the theory developed here to predict the fracture strength of composite laminates with various crack angles.

- Develop a methodology to predict the inherent flaw size at the crack tip before fracture.

THIS PAGE INTENTIONALLY LEFT BLANK

6.0 REFERENCES

1. Adams, D. F. and Mahishi, J.M. "Delamination Micromechanics Analysis", NASA Report, N85-31237, May 1985.

2. Whitney, J.M., "Fracture Analysis of Laminates", Composites Engineered Materials Handbook, ASM International, Volume 1, 2987.

3. Waddoups, M.G., Eisenmann, J.R. and Kaminski, B.E., "Microscopic Fracture Mechanics of Advanced Composites Materials", Journal of Composite Material, Vol. 5, 1971, p.446.

4. Bowie, O.L., "Analysis of an Infinite Plate Containing Radial Cracks Originating from the Boundary of an Internal Circular Hole", Journal of Mathematics and Physics, Vol. 35, 1956, p.60.

5. Adsit, N.R. and Waszczak, J.P. " Fracture Mechanics Correlation of Boron/Aluminum Coupon Containing Stress Risers", ASTM STP 593, 1975.

6. Morris, D.H. and Han, H.T., "Fracture Resistance Characterization of Graphite/Epoxy Composites", Composites Materials: Testing and Design, ASTM, STP 617, pp.5-17, 1976

7. Awerbuch. J., and Han, H.T., "Crack Tip Damage and Fracture Toughness of Boron/Aluminum Composites", Journal of Composite Materials, Vol. 13, April 1979, pp. 82-1078.

8. Poe, C.C.Jr., and Sova, J.A. "Fracture Toughness of Boron/Aluminum Laminates with Various Proportions of 0° and ±45° Plies", NASA TP 1707, 1980.

9. Mar, J.W. and Lin, D.Y., "Fracture Mechanics Correlation for Tensile Failure of Filamentary Composites with Holes", Journal of Aircraft, Vol. 14, p. 703, 1977.

10. Lin, K.Y. and Mar, J.W., "Finite Element Analysis of Stress Intensity factors for Cracks at a Bi-Material Interface", International Journal of Fracture, 12, pp. 521-531, 1976.

11. Bogy, D.B., "On the Plane Elastostatic Problem of a Loaded Crack Terminating at a Material Interface", Journal of Applied Mechanics, Transaction ASME, 38, Series E., No. 4 PP. 911-918, December 1971.

12. Zak, A.R. and Williams, M.L., Journal of Applied Mechanics, 30 Transaction of ASME, 85, Series E. pp. 142-143, March 1963.

13. Irwin G.R. "Analysis of Stresses and Strains Near the end of a crack Traversing a Plate", Journal of Applied Mechanics, Transactions ASME, Vol. 24, 1957

14. Johnson, W.S. and Bigelow, C.A., "Experimental and Analytical Investigation of Fracture Process of Boron/Aluminum Laminates Containing Notches", NASA TP 2187, 1983.

15. Mardell, J.F.Wang, Su-Su, McGaury, J. Frederich, "The Extension of Crack Tip Damage Zones in Fiber Reinforced Plastic Laminates", Journal of Composite Materials, Vol. 9, July 1975.

16. Nuismer, R.J. and Whitney, J.M., "Uniaxial Failure, of Composite Laminates Containing Stress Concentrations", Fracture Mechanics of Composites, ASTM STP 593, American Society for Testing and Materials, Philadelphia, pp. 117-142, 1975.

17. Wu, E.M., "Strength and Fracture of Composites", Fracture and Fatigue, Composite Materials, Vol. 5, 1974.

18. Goree, J.G. and Dharani, R. "Mathematical Modeling of Damage in Unidirectional Composites". NASA Contractor Report 3453, 1981.

19. Mar, J.W. and Lin, K.Y., "Fracture of Boron/Aluminum Composites with Discontinuities", *Journal of Composite Materials*, Vol. 11, Oct. 1977, pp. 405-421.

APPENDIX A

CALCULATION OF THE ORDER OF STRESS SINGULARITY AT A BI-MATERIAL INTERFACE

APPENDIX A

CALCULATION OF THE ORDER OF STRESS SINGULARITY AT A BI-MATERIAL INTERFACE

In the case of a crack, normal to the bi-material interface as shown in figure A-1, the characteristic equation to determine the order of stress singularity is given as follows.[10]:

$$\tau^2(-4\alpha^2 + 4\alpha\beta) + 2\alpha^2 - 2\alpha\beta + 2\alpha - \beta + 1 + (-2\alpha^2 + 2\alpha\beta - 2\alpha + 2\beta)\cos\tau\pi = 0 \qquad \text{(A–1)}$$

where

$$\alpha = \frac{\frac{\mu_1}{\mu_2} - 1}{\eta_1 + 1}$$

$$\beta = \frac{\mu_1(\eta_2 + 1)}{\mu_2(\eta_1 + 1)} \qquad \text{(A-2)}$$

$\eta_1 = 3 - 4\nu_1$, $\eta_2 = 3 - 4\nu_2$ for plane strain

$\eta_1 = (3 - \nu_2)/(1 + \nu_1)$, $\eta_2 = (3 - \nu_2)/(1 + \nu_2)$ for plane stress

μ_1, μ_2 = Shear modulus of medium 1 and 2 respectively

ν_1, ν_2 = Poison's ratio for medium 1 and 2 respectively

The stresses near the crack tip (for $\theta = 0$) can be written as

$$\sigma_x \sim r^{\tau - 1}$$

$$\sigma_y \sim r^{\tau - 1}$$

$$\tau_{xy} \sim r^{\tau - 1} \qquad \text{(A–3)}$$

The order of stress singularity is defined as

$$m = 1 - \tau \qquad \text{(A–4)}$$

By treating the matrix as medium 1, and fiber as medium 2, equations (A-1) to (A-4) are used to calculate the order of singularities for various composite materials as follows:

BORON/ALUMINUM

The properties of boron fiber and aluminum matrix are as follows:

Aluminum:	$\mu_1 = 3.76$ msi, $\nu_1 = .33$
Boron:	$\mu_2 = 26.77$ msi, $\nu_2 = .13$

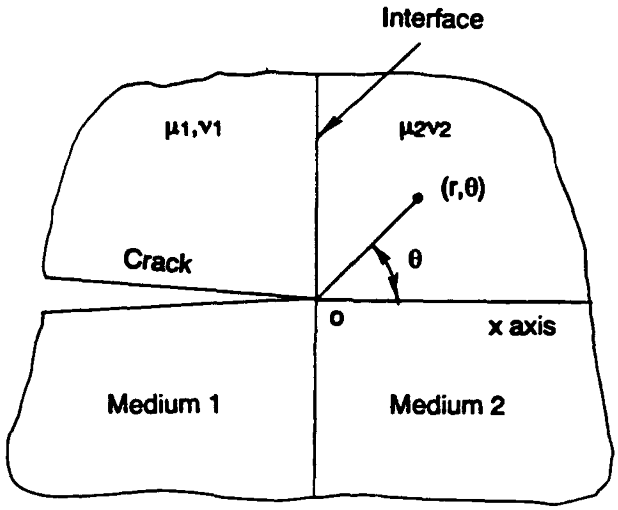

Figure A-1. Crack Normal To The Bi-Material Interface.

Substituting these properties into equations (A-1) and (A-2) for plane stress case, we have the following characteristic equation:

$$.5191\,\tau^2 - .6448\cos\tau\pi - .5204 = 0 \qquad \text{(A-5)}$$

Solving equation (A-5), we have

$$\tau = .653$$

From equation (A-4)

$$m = .347$$

GRAPHITE/EPOXY

For Thornel graphite fiber properties

$$\mu_2 = 4 \text{ msi} \qquad \nu_2 = .2$$

For Epoxy matrix properties

$$\mu_1 = ,19 \text{ msi} \qquad \nu_1 = .35$$

Applying the same procedures as for the Boron/Aluminum Composite, we find

m=.297 for Thornel Graphite/Epoxy

GLASS/EPOXY

For E-type glass fiber,

$$\mu_2 = 4.4 \text{ msi} \qquad \nu_2 = .2$$

For Epoxy matrix,

$$\mu_1 = .17 \text{ msi} \qquad \nu_1 = .35$$

Applying the same procedure as for the Boron/Aluminum composite we find:

m = .289 for E-type Glass/Epoxy

THIS PAGE INTENTIONALLY LEFT BLANK

APPENDIX B

CALCULATION OF $\overline{K}_Q$ AND $\frac{\sigma_N}{\sigma_O}$ FOR VARIOUS COMPOSITE LAMINATES

APPENDIX B

CALCULATION OF $\overline{K}_Q$ AND $\frac{\sigma_N}{\sigma_O}$ FOR VARIOUS COMPOSITE LAMINATES

The following equations were used to calculate $\overline{K}$ and $\frac{\sigma_N}{\sigma_O}$

$$\overline{K} = a_O{}^m \sigma_O \left\{ \left(\frac{Y\sigma_N}{\sigma_O} \right)^{-1/m} - 1 \right\}^{-m} \tag{B-1}$$

$$\frac{\sigma_N}{\sigma_O} = \frac{1}{Y} \left[\frac{1}{1 + \left(\frac{\overline{K}}{\sigma_O} \right)^{-1/m} a_O} \right]^m \tag{B-2}$$

B.1 BORON/ALUMINUM COMPOSITE (M =.347)

B.1.1 Determination of $\overline{K}_Q$ (Tables 1 to 4)

Column 5 of Tables 1 to 4 listed the test results of $\frac{\sigma_N}{\sigma_O}$. Substituting these quantities into equation (B-1), we obtain $\overline{K}$ for various ξ (i.e. $\frac{2a_O}{w}$) values as shown in Column 6 of Tables 1 to 4. $\overline{K}_Q$ is then defined as

$$\overline{K}_Q = \overline{K}_{AVG} = \frac{1}{n} \sum_{i=1}^{n} \overline{K}_i \tag{B-3}$$

Where n = total number of test data, and where $\overline{K}_{AVG}$ rather than $\overline{K}_{LSF}$ is chosen to be $\overline{K}_Q$, the critical stress intensity factor as demonstrated in Figures 3 through 6 in Section 3.2.

B.1.2 Determination Of $\overline{K}_Q$ From Test Data Of Reference 5

Column 4 of Tables B-1 to B-3 shows the test results for various ratios of ξ. Using the same procedures described in the previous section we can obtain $\overline{K}_Q$ for composite laminates with a center hole, double edge notch, and center slit respectively as shown in Column 5 of Table B-1 to Table B-3.

Table B-1. Unidirectional B/Al Composite Laminates With Center Hole.

σ_O = 1470.79 MPa

R_O (mm)	ξ	Y_H	$\left(\frac{\sigma_N}{\sigma_O}\right)_{TEST}$	$\overline{K}$ MPa (mm)$^{.347}$	$\frac{\sigma_N}{\sigma_O}$
1.5875	.25	1.04	.542	1048.31	.601
2.38125	.25	1.04	.521	1149.86	.538
3.175	.25	1.04	.513	1247.19	.495
6.35	.25	1.04	.443	1339.3	.400

$\overline{K}_Q = \overline{K}_{AVG}$ = 1196 MPa (mm)$^{.347}$

$$Y_H = \sqrt{\sec\left(\frac{\pi\xi}{2}\right)}$$

Table B-2. Unidirectional B/Al Composite Laminates With Double Edge Notch.

a_o (mm)	ξ	Y_c / Y_o	$\left(\frac{\sigma_N}{\sigma_o}\right)_{TEST}$	$\overline{K}$ MPa$(mm)^{.343}$	$\frac{\sigma_N}{\sigma_o}$
1.905	.3	1.01	.565	1270.02	.546
2.8575	.3	1.01	.453	1128.47	.489
3.81	.3	1.01	.471	1302.47	.443
7.62	.3	1.01	.338	1156.97	.354

$$K_Q = K_{AVG} = 1214.5 \text{ MPa } (mm)^{.347}$$

$$Yc = (1.98 + .36\,\xi - 2.12\,\xi^2 + 3.42\,\xi^3)/1.77$$

Table B-3. Unidirectional B/Al Composite Laminates With Center Slit.

a_o (mm)	ξ	Y_H	$\left(\frac{\sigma_N}{\sigma_o}\right)_{TEST}$	$\overline{K}$ MPa $(mm)^{.347}$	$\frac{\sigma_N}{\sigma_o}$
3.81	.4	1.11	.431	1160.85	.454
7.62	.4	1.11	.382	1292.61	.362

$$\overline{K}_Q = \overline{K}_{AVG} = 1227 \text{ MPa } (mm)^{.347}$$

$$Y_c = \sqrt{\sec\left(\frac{\pi\,\xi}{2}\right)}$$

Table B-4. Fracture Strength Prediction For B/Al $[0]_{6T}$ With Center Hole.

R_o (mm)	ξ	Y_H	$\overline{K}_Q$ $.347$ MPa(mm)	$\left(\frac{\sigma_N}{\sigma_o}\right)_T$	$\left(\frac{\sigma_N}{\sigma_o}\right)$	Error %
1.59	.0625	1.0	1360	.628	.625	–0.5
3.175	.125	1.01	1360	.538	.510	–5.0
6.35	.125	1.01	1360	.419	.412	–1.7
6.35	.25	1.04	1360	.371	.4	7.9
12.7	.25	1.04	1360	.299	.319	6.7

$$\frac{\sigma_N}{\sigma_o} = \frac{1}{Y}\,(1 + 1.813R_o)^{-.347}$$

B.1.3 Prediction of $\frac{\sigma_N}{\sigma_O}$ for Boron/Aluminum Laminates with Center Hole

From Tables 1 to Table 4, we have $\overline{K}_Q$ for $[0]_{6T}$, $[0_2/\pm45]_s$ and $[0/\pm45]_s$ as 1360 MPa $(mm)^{.347}$, 685.6 MPa $(mm)^{.347}$ and 633.5 MPa $(mm)^{.347}$ respectively. Substituting these quantities into equation (B-2) for $\overline{K}$, we can predict the fracture strength of composite laminates with a center hole as shown in Tables B-4 to B-6. The test data are obtained from Reference 14.

Table B-5. Fracture Strength Prediction For B/Al $[0_2/\pm45]_s$ With Center Hole.

R_0 (mm)	ξ	Y_H	$\overline{K}_Q$	$\left(\frac{\sigma_N}{\sigma_O}\right)_T$	$\left(\frac{\sigma_N}{\sigma_O}\right)$	Error %
1.59	.0625	1.0	685.6	.625	.649	3.8
3.175	.125	1.01	685.6	.525	.533	1.5
16.35	.125	1.01	685.6	.475	.432	–9.2
6.35	.25	1.04	685.6	.450	.420	–6.7
12.7	.25	1.04	685.6	.375	.335	10.0

$$\frac{\sigma_N}{\sigma_o} = \frac{(1+1.56R_o)^{-.347}}{Y_H}$$

Table B-6. Fracture Strength Prediction For B/Al $[0/\pm45]_s$.

a_O (mm)	ξ	Y_H	$\overline{K}_Q$	$\left(\frac{\sigma_N}{\sigma_O}\right)_T$	$\left(\frac{\sigma_N}{\sigma_O}\right)$	Error %
1.59	.0625	1.0	633.5	.792	.756	–4.6
3.175	.125	1.01	633.5	.645	.642	0.
6.35	.125	1.01	633.5	.585	.533	–9.0
6.35	.25	1.04	633.5	.499	.517	3.5
12.7	.25	1.04	633.5	.465	.419	–10.0

$$\frac{\sigma_N}{\sigma_O} = \frac{1}{Y}(1 + .781R_O)^{-.347}$$

B.2 GRAPHITE/EPOXY COMPOSITE (m=.297)

Substituting m=.297 and the test data from Reference 6 as shown in Column 4 of Tables B-7 to B-9, into equation (B.1), we can obtain $\bar{K}$ as listed on Column 5 of the Tables. Then use equation (B-3) to obtain $\bar{K}_Q$.

After obtaining $\bar{K}_Q$, substituting these quantities into equation (B-2), we can obtain $\frac{\sigma_N}{\sigma_0}$ of various ξ for different laminate configurations as shown in Column 6 of Tables B-7 to B-9.

B.3 GLASS/EPOXY COMPOSITES (m=.289)

Substituting m=.289 and the test data from Reference 16, as shown in column 4 of Table B-10, into equation (B-1) we ootain $\bar{K}$ as listed in column 5. $\bar{K}_Q$ can be obtained from equation (B-3). By substituting $\bar{K}_Q$ into equation (B-2), we can obtain $\frac{\sigma_N}{\sigma_0}$ for the composite laminate $[0/\pm45/90]_s$ with both a center crack and a center hole as shown in Column 6 of Tables B-10 and B-11.

Table B-7. Fracture Parameters Of Gr/Ep Laminate $[0/\pm45]_{2s}$ With Center Crack.

a_0 (mm)	ξ	Y	$\left(\frac{\sigma_N}{\sigma_0}\right)_{Test}$	R (MPa mm)	$\left(\frac{\sigma_N}{\sigma_0}\right)$	Error %
2.54	.1	1.01	.56	423	.543	-3.0
5.08	.2	1.026	.46	424	.444	-3.4
7.62	.3	1.054	.38	402	.386	1.6
10.16	.4	1.103	.34	409	.34	0
12.7	.5	1.189	.28	386	.296	5.7

$\bar{K}_Q = \bar{K}_{AVG} = 408.6\ \text{MPa(mm)}^{.297}$

$\sigma_0 = 541$ MPa

Table B-8. Fracture Parameters Of Gr/Ep Laminate $[0/\pm45]_s$ With Center Crack.

a_0 (mm)	ξ	Y	$\left(\frac{\sigma_N}{\sigma_0}\right)_{Test}$	$\bar{K}$ (MPa mm)	$\left(\frac{\sigma_N}{\sigma_0}\right)$	Error %
2.54	.1	1.01	.53	397	.526	0.
5.08	.2	1.026	.44	404	.429	−2.5
7.62	.3	1.054	.39	413	.373	−4.5
10.16	.4	1.103	.33	396	.328	−.6
12.7	.5	1.89	.26	358	.285	9.7

$\bar{K}_Q=\bar{K}_{AVG}=393.5\ \mathrm{MPa(mm)}^{.297}$

$\sigma_0 = 541$ MPa

Table B-9. Fracture Parameters of Gr/Ep Laminate $[0/90/\pm45]_s$ With Center Crack.

a_0 (mm)	ξ	Y	$\left(\frac{\sigma_N}{\sigma_0}\right)_{Test}$	$\bar{K}$ (MPa mm)$^{.289}$	$\left(\frac{\sigma_N}{\sigma_0}\right)$	Error %
2.54	.1	1.01	.69	464	.662	−4.1
5.08	.2	1.026	.57	454	.552	−3.1
7.62	.3	1.054	.47	424	.484	2.9
10.16	.4	1.103	.416	425	.428	2.8
12.7	.5	1.189	.36	422	.373	3.7

$\bar{K}_Q = \bar{K}_{AVG} = 437.7\ \mathrm{MPa(mm)}^{.297}$

$\sigma_0 = 454$ MPa

Table B-10. Fracture Parameters of Gl/Ep $[0/\pm45/90]_s$ with a Center Crack.

a_o (mm)	ξ	Y_c	$\left(\frac{\sigma_N}{\sigma_o}\right)_{Test}$	$\bar{K}$ (MPa mm)$^{.289}$	$\left(\frac{\sigma_N}{\sigma_o}\right)$	Error %
1.45	.11	1.01	.707	283.3	.708	0.
3.86	.30	1.054	.578	305	.530	-8.4
7.37	.29	1.05	.440	268.8	.448	1.0
12.4	.33	1.06	.338	239.4	.382	13.0

$\bar{K}_Q = \bar{K}_{AVG} = 274$ MPa(mm)$^{.289}$

$\sigma_0 = 320$ MPA

Table B-11. Fracture Strength Prediction of Gl/Ep $[0/\pm45/90]_s$ with a Center Hole.

R_o (mm)	ξ	Y_H	$\bar{K}_Q$ (MPa mm)$^{.289}$	$\left(\frac{\sigma_N}{\sigma_o}\right)_{Test}$	$\left(\frac{\sigma_N}{\sigma_o}\right)$	Error %
1.27	.1	1.01	274	.696	.709	1.8
3.81	.3	1.054	274	.511	.530	3.6
7.62	.3	1.054	274	.44	.442	.5
12.7	.33	1.06	274	.375	.383	2.0

APPENDIX C
ANALYTICAL RESULTS OF ANISOTROPIC MODEL

APPENDIX C. ANALYTICAL RESULTS OF ANISOTROPIC MODEL.

INHERENT FLAW CONCEPT
B/AL $(\pm 45/0_2)_s$ EXPONENT = 0.500
UNNOTCHED STRENGTH = 910.5 C_o = 1.505519

a	$\frac{2a}{w}$	Y	$\left(\frac{\sigma_N}{\sigma_o}\right)^{exp-1}$	$\left(\frac{\sigma_N}{\sigma_o}\right)$ TEST	$\left(\frac{\sigma_N}{\sigma_o}\right)$ CALC	%ERR
1.25	0.05	1.00579E+00	1.57989E+00	6.19000E-01	7.34908E-01	18.7
2.55	0.05	1.00590E+00	2.54504E+00	5.28000E-01	6.05709E-01	14.7
2.55	0.10	1.01151E+00	2.46633E+00	5.31000E-01	6.02351E-01	13.4
5.10	0.10	1.01151E+00	4.46234E+00	4.23000E-01	4.71975E-01	11.6
7.60	0.30	1.05343E+00	5.91474E+00	3.61000E-01	3.85999E-01	6.9
12.70	0.50	1.18275E+00	1.09092E+01	2.45000E-01	2.75246E-01	12.3
15.25	0.30	1.05379E+00	1.04046E+01	2.81000E-01	2.84453E-01	1.2
25.40	0.50	1.18275E+00	1.66938E+01	2.01000E-01	2.00000E-01	0.5

INHERENT FLAW CONCEPT
B/AL $(0/\pm 45)_s$ EXPONENT = 0.500
UNNOTCHED STRENGTH = 581.4 C_o = 2.836446

a	$\frac{2a}{w}$	Y	$\left(\frac{\sigma_N}{\sigma_o}\right)^{exp-1}$	$\left(\frac{\sigma_N}{\sigma_o}\right)$ TEST	$\left(\frac{\sigma_N}{\sigma_o}\right)$ CALC	%ERR
0.65	0.07	1.00787E+00	4.35914E-01	8.28000E-01	8.94933E-01	8.1
1.25	0.05	1.00579E+00	5.60115E-01	7.96000E-01	8.28334E-01	4.1
2.55	0.05	1.00590E+00	1.08791E+00	6.88000E-01	7.21407E-01	4.9
2.55	0.10	1.01151E+00	8.34061E-01	7.30000E-01	7.17407E-01	1.7
5.10	0.10	1.01151E+00	1.54259E+00	6.20000E-01	5.91022E-01	4.7
7.60	0.30	1.05343E+00	3.29595E+00	4.58000E-01	4.94887E-01	8.1
12.70	0.50	1.18275E+00	5.60423E+00	3.29000E-01	3.61259E-01	9.8
15.25	0.30	1.05379E+00	4.27950E+00	4.13000E-01	3.75800E-01	9.0
25.40	0.50	1.18275E+00	8.73365E+00	2.71000E-01	2.67972E-01	1.1

INHERENT FLAW CONCEPT
B/AL $(0_2/\pm45)_S$ EXPONENT = 0.500
UNNOTCHED STRENGTH = 800.1 C_0 = 1.933202

a	$\frac{2a}{w}$	Y	$\left(\frac{\sigma_N}{\sigma_0}\right)^{exp-1}$	$\left(\frac{\sigma_N}{\sigma_0}\right)$ TEST	$\left(\frac{\sigma_N}{\sigma_0}\right)$ CALC	%ERR
0.25	0.03	1.00319E+00	2.88986E-01	8.78000E-01	9.38016E-01	6.8
0.65	0.07	1.00787E+00	6.09814E-01	7.82000E-01	8.58330E-01	9.8
1.25	0.05	1.00579E+00	9.01570E-01	7.21000E-01	7.74815E-01	7.5
2.55	0.05	1.00590E+00	1.94803E+00	5.79000E-01	6.52813E-01	12.7
2.55	0.10	1.01151E+00	1.99769E+00	5.71000E-01	6.49194E-01	13.7
5.10	0.10	1.02251E+00	3.53966E+00	4.64000E-01	5.18313E-01	11.7
7.60	0.30	1.05343E+00	4.77558E+00	3.95000E-01	4.27478E-01	8.2
12.70	0.50	1.18275E+00	8.52167E+00	2.74000E-01	3.07310E-01	12.2
15.25	0.30	1.05379E+00	7.76124E+00	3.20600E-01	3.18297E-01	0.7
25.40	0.50	1.18275E+00	1.26673E+01	2.28700E-01	2.24854E-01	1.7

INHERENT FLAW CONCEPT
B/AL $(0)_{6T}$ EXPONENT = 0.500
UNNOTCHED STRENGTH = 1672 C_0 = 2.080114

a	$\frac{2a}{w}$	Y	$\left(\frac{\sigma_N}{\sigma_0}\right)^{exp-1}$	$\left(\frac{\sigma_N}{\sigma_0}\right)$ TEST	$\left(\frac{\sigma_N}{\sigma_0}\right)$ CALC	%ERR
0.25	0.03	1.00319E+00	4.85014E-01	8.18000E-01	9.41832E-01	15.1
0.65	0.07	1.00787E+00	1.10108E+00	6.84500E-01	8.66060E-01	26.5
1.25	0.05	1.00579E+00	1.82059E+00	5.92000E-01	7.85788E-01	32.7
2.55	0.05	1.00590E+00	1.93787E+00	5.80000E-01	6.66334E-01	14.9
2.55	0.10	1.01151E+00	2.17303E+00	5.55000E-01	6.62640E-01	19.4
5.10	0.10	1.01151E+00	3.46239E+00	4.68000E-01	5.32118E-01	13.7
7.60	0.30	1.05343E+00	4.62366E+00	4.00300E-01	4.40046E-01	9.9
12.70	0.50	1.18275E+00	6.44820E+00	3.09800E-01	3.17184E-01	2.4
15.25	0.30	1.05379E+00	8.84757E+00	3.02400E-01	3.28768E-01	8.7
25.40	0.50	1.18275E+00	1.22812E+01	2.32000E-01	2.32617E-01	0.3

DISTRIBUTION LIST

No. of Copies

Kaman Aerospace.. 1
Attn: Mr. A. Falcone
Old Windsor Road
Bloomfield, CT 06002

NAVAIRDEVCEN..1
Tom Hess, Code 60C1

NAVAIRDEVCEN.. 3
Code 6064

NAVAIRDEVCEN.. 2
Code 8131

NAVAIRDEVCEN..25
Code 6043

DISTRIBUTION LIST

No. of Copies

Rockwell International/North American Aircraft Division............. 1
Attn: Mr. W. O'Brien
P.O. Box 92098
Los Angeles, CA 90009

Rockwell International/North American Aircraft Division............. 1
Advanced Technology Program Development
Attn: Dr. Lackman
P.O. Box 92098
Los Angeles, CA 90009

Rockwell International/North American Aircraft Operations............ 1
Attn: Technical Library
P.O. Box 582808
Tulsa, OK 74158

Rockwell International/North American Aircraft Operations............ 1
Attn: Mr. G. Sherrick, Engineering Research and Technology
P.O. Box 582808
Tulsa, OK 74158

Rockwell International/North American Aircraft Operations............ 1
Attn: Mr. M. Whitehead
P.O. Box 582808
Tulsa, OK 74158

Rockwell International/North American Aircraft Operations............ 1
Attn: Mr. F. Kaufman
P.O. Box 582808
Tulsa, OK 74158

Sikorsky Aircraft... 1
Attn: Technical Library
North Main Street
Stratford, CT 06601-1381

Sikorsky Aircraft... 1
Attn: Mr. Samuel P. Garbo, MS S314A2
North Main Street
Stratford, CT 06601-1381

Sikorsky Aircraft... 1
Attn: Mr. T. Cook
North Main Street
Stratford, CT 06601-1381

DISTRIBUTION LIST

No. of Copies

McDonnell-Douglas Astronautics.................................... 1
Attn: Mr. C. M. Roe
5301 Bolsa Avenue
Huntington Beach, CA 92647

Northrop Aircraft Corporation..................................... 1
Attn: Technical Library
One Northrop Avenue
Hawthorne, CA 90250

Northrop Aircraft Corporation..................................... 1
Attn: Mr. D. Boldi
One Northrop Avenue
Hawthorne, CA 90250

Northrop Aircraft Corporation..................................... 1
Attn: Dr. M. Ratwani
One Northrop Avenue
Hawthorne, CA 90250

Northrop Aircraft Corporation..................................... 1
Attn: Mr. B. Butler
One Northrop Avenue
Hawthorne, CA 90250

Northrop Aircraft Corporation..................................... 1
Attn: Mr. R. Whitehead, Structures Research
One Northrop Avenue
Hawthorne, CA 90250

Rockwell International/North American Aircraft Division.............. 1
Attn: Technical Library
P.O. Box 92098
Los Angeles, CA 90009

Rockwell International/North American Aircraft Division.............. 1
Attn: Mr. G. Stewart, Advanced Structures Engineering
P.O. Box 92098
Los Angeles, CA 90009

Rockwell International/North American Aircraft Division.............. 1
Attn: Mr. A. Sanders
P.O. Box 92098
Los Angeles, CA 90009

DISTRIBUTION LIST

No. of Copies

McDonnell-Douglas Corporation.. 1
Douglas Aircraft Company
Attn: Mr. A. Hawley, Dept. ELH, M/S 212-10
3855 Lakewood Blvd.
Long Beach, CA 90846

McDonnell-Douglas Corporation.. 1
Douglas Aircraft Company
Attn: Mr. R. Petty, Dept. 1L7, M/S 35-98
3855 Lakewood Blvd.
Long Beach, CA 90846

McDonnell-Douglas Corporation.. 1
Douglas Aircraft Company
Attn: Mr. Clifford Y. Kam, Dept. EL8, M/S 212-20
Long Beach, CA 90846

McDonnell-Douglas Helicopter Company............................... 1
Attn: Technical Library
Culver City, CA 90230

McDonnell-Douglas Helicopter Company............................... 1
Attn: Mr. R. M. Verette
Culver City, CA 90230

McDonnell-Douglas Helicopter Company............................... 1
Attn: Technical Library
5000 E. McDowell Road
Mesa, AZ 85205

McDonnell-Douglas Helicopter Company............................... 1
Attn: Mr. J. K. Sen
MS 338, Bldg. 530
5000 E. McDowell Road
Mesa, AZ 85205

McDonnell-Douglas Helicopter Company............................... 1
Attn: Mr. S. Guymon, MS B337
5000 E. McDowell Road
Mesa, AZ 85205

McDonnell-Douglas Astronautics... 1
Attn: Technical Library
5301 Bolsa Avenue
Huntington Beach, CA 92647

DISTRIBUTION LIST

No. of Copies

LTV Aerospace and Defense Company.................................... 1
Vought Missiles and Advanced Programs Division
Attn: C. Foreman, Engineering Project Manager
P.O. Box 655907
Dallas, TX 75265-5907

LTV Aerospace and Defense Company.................................... 1
Vought Missiles and Advanced Programs Division
Attn: Mr. R. Knight, MS-TH-83
P.O. Box 650003
Dallas, TX 75265-0003

LTV Aircraft Product Group... 1
Structures Research and Development
Attn: Mr. R. Ely, Technical Project Manager
P.O. Box 655907
Dallas, TX 75265-5907

McDonnell-Douglas Corporation.. 1
Attn: Technical Library
P.O. Box 516
St. Louis, MO 63166

McDonnell-Douglas Corporation.. 1
Attn: Mr. C. Pingle, Dept. 337, M/S 0644324
P.O. Box 516
St. Louis, MO 63166

McDonnell-Douglas Corporation.. 1
Attn: Mr. D. J. Dorr, Dept. 390, M/S 1021310
P.O. Box 516
St. Louis, MO 63166

McDonnell-Douglas Corporation.. 1
Attn: Mr. C. Saff, Dept. 337, M/S 0341160
P.O. Box 516
St. Louis, MO 63166

McDonnell-Douglas Corporation.. 1
Attn: Mr. T. Hinkel, Dept. 334, M/S 0643063
P.O. Box 516
St. Louis, MO 63166

McDonnell-Douglas Corporation.. 1
Douglas Aircraft Company
Attn: Technical Library
Mail Code 212-10
Long Beach, CA 90846

DISTRIBUTION LIST

No. of Copies

Lockheed Aeronautic Systems Company.................................. 1
Attn: Mr. E. K. Walker
P.O. Box 551 - Dept. 76-02, B63, Plt. A1
Burbank, CA 91520

Lockheed Aeronautic Systems Company.................................. 1
Attn: C. F. Griffin, Dept. 76-24
Advanced Structures Technology Dept.
Burbank, CA 91520

Lockheed-Georgia Company.. 1
Attn: Technical Library
86 South Cobb Drive
Marietta, GA 30063

Lockheed-Georgia Company.. 1
Attn: Mr. L. R. Meade, MS 399
86 South Cobb Drive
Marietta, GA 30063

Lockheed-Georgia Company.. 1
Attn: Technical Information
Dept. 72-34, Zone 26
Marietta, GA 30063

Lockheed-Missile and Space Company.................................. 1
Attn: Technical Library
1111 Lockheed Way
Sunnyvale, CA 94088

Lockheed-Missile and Space Company.................................. 1
Attn: Mr. J. A. Bailie
P.O. Box 504, Dept. 81-12, B154
1111 Lockheed Way
Sunnyvale, CA 94088

LTV Aerospace and Defense Company.................................... 1
Vought Aeroproducts Division
Attn: Technical Library
P.O. Box 655907
Dallas, TX 75265-5907

LTV Aerospace and Defense Company.................................... 1
Vought Aeroproducts Division
Attn: Mr. J. Pimm, MS 194-51
P.O. Box 655907
Dallas, TX 75265-5907

DISTRIBUTION LIST

	No. of Copies
General Electric Company Attn: Dr. B. Rodini P.O. Box 8555-M4018 Philadelphia, PA 19101	1
Grumman Aerospace Corporation Attn: Technical Library South Oyster Bay Road Bethpage, Long Island, NY 11714	1
Grumman Aerospace Corporation Attn: Mr. R. Hadcock, Advanced Materials South Oyster Bay Road Bethpage, Long Island, NY 11714	1
Grumman Aerospace Corporation Attn: Mr. J. Bruno, B44-35 South Oyster Bay Road Bethpage, Long Island, NY 11714	1
Grumman Aerospace Corporation Attn: Mr. S. Dastin South Oyster Bay Road Bethpage, Long Island, NY 11714	1
Lockheed Aeronautical Systems Company Attn: Technical Library P.O. Box 551 Burbank, CA 91520	1
Lockheed Aeronautical Systems Company Attn: C. W. Schneider D/70-03, B-369, P/B-6 P.O. Box 551 Burbank, CA 91520	1
Lockheed Aeronautic Systems Company Attn: Mr. D. E. Pettit Rye Canyon Research Lab Burbank, CA 91520	1
Lockheed Aeronautic Systems Company Attn: Mr. R. C. Young Rye Canyon Research Lab Burbank, CA 91520	1

DISTRIBUTION LIST

No. of Copies

General Dynamics/Fort Worth Division................................ 1
Attn: Mr. T. Kearns, MS 6217
P.O. Box 748
Fort Worth, TX 76101

General Dynamics/Fort Worth Division................................ 1
Attn: Mr. J. A. Fant
P.O. Box 748 - MZ 2884
Fort Worth, TX 76101

General Dynamics/Fort Worth Division................................ 1
Attn: Dr. G. Law, Composite Structures Certification
P.O. Box 748
Fort Worth, TX 76101

General Electric Company.. 1
Attn: Technical Library
1 Neumann Way
Cincinnati, OH 45215

General Electric Company.. 1
Attn: Mr. S. Johnson
1 Neumann Way
Cincinnati, OH 45215

General Electric Company.. 1
Attn: Mr. A. W. Kim
1 Neumann Way
Cincinnati, OH 45215

General Electric Company.. 1
Attn: Technical Library
P.O. Box 8555
Philadelphia, PA 19101

General Electric Company.. 1
Attn: Mr. A. Garber
P.O. Box 8555-M4018
Philadelphia, PA 19101

General Electric Company.. 1
Attn: Mr. C. Zweben
P.O. Box 8555-M4018
Philadelphia, PA 19101

DISTRIBUTION LIST

No. of Copies

Boeing Military Aircraft Company.................................... 1
Attn: Mr. J. Avery
P.O. Box 20746
Wichita, KS 67277-7730

Boeing Military Aircraft Company.................................... 1
Attn: Mr. R. Waner
P.O. Box 20746
Wichita, KS 67277-7730

Boeing Military Airplane Company.................................... 1
Attn: Mr. J. Luding, MS K3216
P.O. Box 20746
Wichita, KS 67277-7730

Boeing Military Airplane Company.................................... 1
Attn: Mr. R. M. Mayle, MS K06-72
P.O. Box 20746
Wichita, KS 67277-7730

General Dynamics/Convair Division.................................... 1
Space Systems Division
Attn: Technical Library
P.O. Box 85990
San Diego, CA 92138

General Dynamics/Convair Division.................................... 1
Space Systems Division
Attn: Craig Rix, MZ-23-8443
P.O. Box 85990
San Diego, CA 92138

General Dynamics/Convair Division.................................... 1
Space Systems Division
Attn: Mr. D. R. Dunbar
P.O. Box 85990
San Diego, CA 92138

General Dynamics/Fort Worth Division................................ 1
Attn: Technical Library
P.O. Box 748
Fort Worth, TX 76101

General Dynamics/Fort Worth Division................................ 1
Attn: Mr. B. Smith
P.O. Box 748
Fort Worth, TX 76101

DISTRIBUTION LIST

No. of Copies

Boeing Helicopter Company.. 1
Attn: Mr. D. Hart
P.O. Box 16858
Philadelphia, PA 19142

Boeing Helicopter Company.. 1
Attn: Mr. R. L. Pinckney
P.O. Box 16858
Philadelphia, PA 19142

Boeing Helicopter Company.. 1
Attn: Mr. C. Albrecht, MS P32-38
P.O. Box 16858
Philadelphia, PA 19142

Boeing Helicopter Company.. 1
Attn: Mr. Brian Lake, MS P30-18
P.O. Box 16858
Philadelphia, PA 19142

Boeing Company... 1
Attn: Technical Library
P.O. Box 3707
Seattle, WA 98124-2207

Boeing Company... 1
Attn: Mr. R. Horton
P.O. Box 3707-MS 3304
Seattle, WA 98124-2207

Boeing Company... 1
Attn: Mr. M. Cohodas
P.O. Box 3707, MS 4A-16
Seattle, WA 98124-2207

Boeing Company... 1
Attn: Mr. J. Quinlivan
P.O. Box 3707, MS 6N-21
Seattle, WA 98124-2207

Boeing Military Aircraft Company................................... 1
Attn: Technical Library
P.O. Box 20746
Wichita, KS 67277-7730

DISTRIBUTION LIST

	No. of Copies
AVCO Specialty Materials - Textron Attn: Mr. William F. Grant Specialty Materials Division 2 Industrial Avenue Lowell, MA 01851	1
AVCO Specialty Materials - Textron Attn: J. Hemshaw Specialty Materials Division 2 Industrial Avenue Lowell, MA 01851	1
Beech Aircraft Corporation Attn: Mr. M. B. Goetz Claypool Bldg., Office 300 4130 Linden Avenue Dayton, OH 45432	1
Beech Aircraft Corporation Attn: Mr. M. P. Djuric Kellogg St. and Webb Road Wichita, KS 67201	1
Bell Helicopter/Textron Inc. Attn: Technical Library P.O. Box 482 Fort Worth, TX 76101	1
Bell Helicopter/Textron Inc. Attn: Mr. D. Reisdorfer P.O. Box 482 Fort Worth, TX 76101	1
Bell Helicopter/Textron Inc. Attn: Mr. M. K. Stevenson P.O. Box 482 Fort Worth, TX 76101	1
Boeing Helicopter Company Boeing Defense and Space Group Attn: Dr. C. K. Gunther P.O. Box 16858, MS P30-30 Philadelphia, PA 19142-0858	1
Boeing Helicopter Company Attn: Technical Library P.O. Box 16858 Philadelphia, PA 19142	1

DISTRIBUTION LIST

No. of Copies

Commander.. 1
Naval Aviation Depot
Attn: J. Gresham, Code 35210
MCAS, Cherry Point, NC 28533-5030

Commander.. 1
Naval Aviation Depot
Attn: M. Linn, Code 340
NAS, Jacksonville, FL 32212-0016

Commander.. 1
Naval Aviation Depot
Attn: J. Deans, Code 31310, Bldg. V88
NAS, Norfolk, VA 23511-5899

Commander.. 1
Naval Aviation Depot
Attn: H. Jarrett, Code 32220
NAS, Norfolk, VA 23511-5899

Commander.. 1
Naval Aviation Depot
Attn: H. Sommerfleck, Code 36030
NAS, Norfolk, VA 23511-5899

Commanding Officer... 1
Naval Aviation Depot
Attn: D. Perl, Code 343
NAS, North Island, San Diego, CA 92135-5112

Commanding Officer... 1
Naval Aviation Depot
Attn: M. Williams, Code 31327
NAS, North Island, San Diego, CA 92135-5112

Commanding Officer... 1
Naval Aviation Depot
Attn: D. Knapp, Code 342
NAS, Pensacola, FL 32508-5300

Commander.. 1
United States Naval Academy
Attn: Mechanical Engineering Dept.
Annapolis, MD 21402

DISTRIBUTION LIST

No. of Copies

Commanding Officer.. 1
U.S. Army R&T Laboratory (ARRADCOM)
Attn: K. Abelson
Building 182
Dover, NJ 07801

Commanding Officer.. 1
U.S. Army R&T Laboratory (ARRADCOM)
Attn: R. Bonk
Building 182
Dover, NJ 07801

Commanding Officer.. 1
U.S. Army Applied Technology Lab
Attn: G. McAllister
USARTL, (AVRADCOM)
Fort Eustis, VA 23604-5418

Commanding Officer.. 1
U.S. Army Applied Technology Lab
Attn: J. Waller
USARTL, (AVRADCOM)
Fort Eustis, VA 23604-5418

NASA Headquarters... 1
Attn: G. Seidel
OAST-Code RM
Washington, D.C. 20546

Administrator... 1
National Aeronautics and Space Administration
Attn: Airframes Branch, FS 120
Washington, D.C. 20546

Administrator... 1
National Aeronautics and Space Administration
Langley Research Center
Attn: Dr. C. P. Blankenship, M/S-188M
Hampton, VA 23365-5225

Administrator... 1
National Aeronautics and Space Administration
Langley Research Center
Attn: Mr. C. E. Harris, MS 188E
Hampton, VA 23365-5225

DISTRIBUTION LIST

No. of Copies

Commander.. 1
David Taylor Research Center
Attn: A. Macander, Code 1720
Bethesda, MD 20084

Commander.. 1
David Taylor Research Center
Attn: E. T. Camponeschi, Code 2844
Annapolis, MD 21402

Commander.. 1
David Taylor Research Center
Attn: R. Crane, Code 2844
Annapolis, MD 21402

Commander.. 1
David Taylor Research Center
Attn: H. Edelstein, Code 2870
Annapolis, MD 21401

Commander.. 1
Naval Surface Weapons Center
Attn: Dr. J. M. Augl
10901 New Hampshire Avenue
Silver Spring, MD 20903-5000

Commander.. 1
Naval Surface Weapons Center
Attn: Dr. J. Goff, R34
White Oak Laboratory
Silver Spring, MD 20910

Commander.. 1
Naval Aviation Depot
Attn: N. Amdur, Code 342/N
NAS, Alameda, CA 94501

Commander.. 1
Naval Aviation Depot
Attn: J. Meyers, Code 35110
MCAS, Cherry Point, NC 28533-5030

Commander.. 1
Naval Aviation Depot
Attn: J. Fuss, Code 35430
MCAS, Cherry Point, NC 28533-5030

DISTRIBUTION LIST

No. of Copies

Commander.. 1
Naval Air Systems Command
Attn: AIR-53022
Washington, D.C. 20361

Commander.. 1
Naval Air Systems Command
Attn: AIR-53023
Washington, D.C. 20361

Commander.. 1
Naval Air Systems Command
Attn: AIR-5304
Washington, D.C. 20361

Commander.. 1
Naval Air Systems Command
Attn: AIR-530T
Washington, D.C. 20361

Commander.. 1
Naval Sea Systems Command
Attn: Sea-05R
Washington, D.C. 20362-5101

Commander.. 1
Naval Weapons Center
Attn: K. Bailey, Code 338
China Lake, CA 93355

Commander.. 1
Naval Weapons Center
Attn: J. E. Diamond, Code 338
China Lake, CA 93355

Commanding Officer.. 1
Naval Ship Engineering Center
Attn: NSEC 6101E
Arlington, VA 20360

Commander.. 1
David Taylor Research Center
Attn: R. Rockwell, Code 1720-6
Bethesda, MD 20084

DISTRIBUTION LIST

	No. of Copies
Office of Naval Technology Attn: W. King, ONT-212 800 N. Quincy Street Arlington, VA 22217	1
Office of Naval Research Attn: A. K. Vasudevan, Code 1216 800 N. Quincy Street Arlington, VA 22217	1
Office of Naval Research Attn: Y. Rajapakse, Code 1132SM 800 N. Quincy Street Arlington, VA 22217	1
Director Naval Research Laboratory Attn: Dr. R. Badaliance 4555 Overlook Avenue, S.W. Washington, D.C. 20375	1
Director Naval Research Laboratory Attn: Dr. I. Wolock, Code 6383 4555 Overlook Avenue, S.W. Washington, D.C. 20375-5000	1
Director Naval Research Laboratory Attn: C. Poranski, Code 6122 4555 Overlook Avenue, S.W. Washington, D.C. 20375-5000	1
Commander Naval Air Systems Command Attn: AIR-530 Washington, D.C. 20361	1
Commander Naval Air Systems Command Attn: AIR-5302 Washington, D.C. 20361	1
Commander Naval Air Systems Command Attn: AIR-53021 Washington, D.C. 20361	1

DISTRIBUTION LIST

	No. of Copies
Administrator National Aeronautics and Space Administration George C. Marshall Space Flight Center Attn: Technical Library Huntsville, AL 35812	1
Administrator National Aeronautics and Space Administration Lewis Research Center Attn: Dr. C. Chamis, MS-49-6 21000 Brookpark Road Cleveland, OH 44153	1
Administrator National Aeronautics and Space Administration Lewis Research Center Attn: M. Hershberg, MS 49-6 21000 Brookpark Road Cleveland, OH 44153	1
Administrator National Aeronautics and Space Administration Lewis Research Center Attn: Technical Library 21000 Brookpark Road Cleveland, OH 44153	1
Administrator Defense Technical Information Center Bldg. #5, Cameron Station Alexandria, VA 22314	2
Federal Aviation Administration Attn: Mr. J. R. Soderquist, AIR-103 800 Independence Avenue, S.W. Washington, D.C. 20591	1
Federal Aviation Administration Attn: Mr. L. Neri, Code ACD-210 Technical Center Atlantic City, NJ 08405	1
Federal Adviation Administration Attn: C. Caiafa, Code ACT-330 Technical Center Atlantic City, NJ 08405	1

DISTRIBUTION LIST

No. of Copies

Administrator.. 1
National Aeronautics and Space Administration
Langley Research Center
Attn: Dr. J. Starnes, MS 190
Hampton, VA 23365-5225

Administrator.. 1
National Aeronautics and Space Administration
Langley Research Center
Attn: Dr. M. Mikulas, Code MS 190
Hampton, VA 23365-5225

Administrator.. 1
National Aeronautics and Space Administration
Langley Research Center
Attn: Mr. W. T. Freeman, MS 243
Hampton, VA 23365-5225

Administrator.. 1
National Aeronautics and Space Administration
Langley Research Center
Attn: Mr. J. W. Deaton, MS 188A
Hampton, VA 23365-5225

Administrator.. 1
National Aeronautics and Space Administration
Langley Research Center
Attn: Mr. J. Davis, MS 243/STPO
Hampton, VA 23365-5225

Administrator.. 1
National Aeronautics and Space Administration
Langley Research Center
Attn: Dr. R. Price
Hampton, VA 23365-5225

Administrator.. 1
National Aeronautics and Space Administration
Langley Research Center
Attn: Dr. G. L. Roderick
Hampton, VA 23365-5225

Administrator.. 1
National Aeronautics and Space Administration
George C. Marshall Space Flight Center
Attn: R. Schwinghamer, S&E-ASTN-M
Huntsville, AL 35812

DISTRIBUTION LIST

	No. of Copies
Commanding Officer Warner Robbins Ai·· Logistics Command Attn: T. F. Christian, MMSRD Robbins Air Force Base, GA 30198	1
Commanding Officer Warner Robbins Air Logistics Command Attn: W. Schweinberg, MMTRC Robbins Air Force Base, GA 30198	1
Commanding Officer Picatinny Arsenal PLASTEC Attn: Librarian, Code DRDAR-SCM-0, Bldg. 351N Dover, NJ 07801	1
Commanding Officer U.S. Army Air Mobility R&D Lab Attn: H. Reddick Fort Eustis, VA 23604	1
Commanding Officer U.S. Army Aviation Applied Technology Directorate Attn: T. E. Condon SAVRT/TY-ASR Fort Eustis, VA 23604-5577	1
Commanding Officer U.S. Army Aviation Applied Technology Directorate Attn: Drew Orlino SAVRT/TY-ATS Fort Eustis, VA 23604-5577	1
Commanding Officer U.S. Army Materials and Mechanical Research Center Attn: D. Oplinger, SLCMT-MS Watertown, MA 02171-0001	1
Commanding Officer U.S. Army Research Office Durham, NC 27701	1
Commanding Officer U.S. Army R&T Laboratory (AVRADCOM) Attn: F. Immen, Code DAVDL-AS-MS-207-5 Ames Research Center Moffett Field, CA 94035	1

DISTRIBUTION LIST

No. of Copies

Commanding Officer.. 1
Wright Research and Development Center
Attn: FIBC/C. Ramsey
Wright Patterson Air Force Base, OH 45433-6553

Commanding Officer.. 1
Wright Research and Development Center
Attn: FIBEC/Dr. G. Sendeckyj
Wright Patterson Air Force Base, OH 45433-6553

Commanding Officer.. 1
Wright Research and Development Center
Attn: FIBR/H. F. Wolfe
Wright Patterson Air Force Base, OH 45433-6553

Commanding Officer.. 1
Wright Research and Development Center
Attn: FIBA/L. Kelly
Wright Patterson Air Force Base, OH 45433-6553

Commanding Officer.. 1
Wright Research and Development Center
Attn: MLBM/Dr. J. Whitney
Wright Patterson Air Force Base, OH 45433-6553

Commanding Officer.. 1
Wright Research and Development Center
Attn: MLSE/S. Fecheck
Wright Patterson Air Force Base, OH 45433-6553

Commanding Officer.. 1
Wright Research and Development Center
Attn: MLBM/Dr. M. Knight
Wright Patterson Air Force Base, OH 45433-6553

Commanding Officer.. 1
Wright Research and Development Center
Attn: MLB/F. Cherry
Wright Patterson Air Force Base, OH 45433-6553

Commanding Officer.. 1
Wright Research and Development Center
Attn: MLSE/T. Reinhart
Wright Patterson Air Force Base, OH 45433-6553

Commanding Officer.. 1
Wright Research and Development Center
Attn: MLTN/R. C. Tomashot
Wright Patterson Air Force Base, OH 45433-6553

DISTRIBUTION LIST

No. of Copies

Commander.. 1
U.S. Naval Postgraduate School
Attn: Professor R. Ball
Monterey, CA 93943

Commander.. 1
U.S. Naval Postgraduate School
Attn: Professor M. H. Bank, Code 67BP
Monterey, CA 93943

Commander.. 1
U.S. Naval Postgraduate School
Attn: Professor K. Challenger
Monterey, CA 93943

Commander.. 1
U.S. Naval Postgraduate School
Attn: Technical Library
Monterey, CA 93943

Commander.. 1
U.S. Naval Postgraduate School
Attn: Dr. E. Robert Wood, Code 67
Monterey, CA 93943

Department of the Air Force.. 1
Attn: Dr. M. Salkind
Building 410
Boiling Air Force Base
Washington, D.C. 20331

Department of the Air Force.. 1
Attn: Dr. J. Amos
Building 410
Boiling Air Force Base
Washington, D.C. 20331

Commanding Officer... 1
Wright Research and Development Center
Attn: FIBA/W. Goesch
Wright Patterson Air Force Base, OH 45433-6553

Commanding Officer... 1
Wright Research and Development Center
Attn: FIB/R. Bader
Wright Patterson Air Force Base, OH 45433-6553